

**SYNTHESIS AND CHARACTERIZATION OF  
HIGHLY DISPERSED NICKEL-BASED  
CATALYSTS FOR ALKALINE DIRECT  
METHANOL FUEL CELLS**

BY

**OLANREWAJU SULEIMAN OLAKUNLE**

A Thesis Presented to the  
DEANSHIP OF GRADUATE STUDIES

**KING FAHD UNIVERSITY OF PETROLEUM & MINERALS**

DHAHRAN, SAUDI ARABIA

In Partial Fulfillment of the  
Requirements for the Degree of

**MASTER OF SCIENCE**

In

**CHEMISTRY**

**DECEMBER 2014**

KING FAHD UNIVERSITY OF PETROLEUM & MINERALS  
DHAHRAN 31261, SAUDI ARABIA

DEANSHIP OF GRADUATE STUDIES

This thesis, written by **OLANREWAJU SULEIMAN OLAKUNLE** under the direction of his thesis advisor and approved by his thesis committee, has been presented to and accepted by the Dean of Graduate Studies, in partial fulfillment of the requirements for the degree of **MASTER OF SCIENCE IN CHEMISTRY**.

Thesis Committee



Dr. Abdalla M. Abulkibash (Advisor)



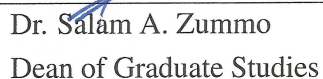
Dr. Amir Al-Ahmed (Member)

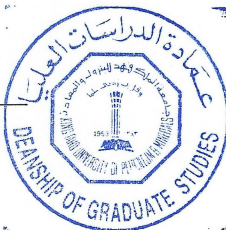


Dr. Abdulrahman Al-Betar (Member)



Dr. Abdulaziz Al-Saadi  
Department Chairman

  
Dr. Salam A. Zummo  
Dean of Graduate Studies



22/3/15

Date

©Olanrewaju Suleiman Olakunle  
2014

## *Dedication*

*To the blessed memory of my late father, Chief L.L Lakunle and to those  
that toil day and night to ensure that I become successful in life..*



# ACKNOWLEDGMENTS

All thanks and adoration to Almighty Allah, the creator of all creatures for making it possible for the successful completion of my MS degree program. I am especially indebted to my beloved mum (Hajia Mulikat Adunni) and grandmum (Hajia Aishat Gbadamosi) for all their effort in supporting me up to date. I sincerely submit that all my successes and achievements, by the Will of Allah (SWT) is a result of their commitment, patience, encouragements and support.

With deep sense of gratitude and appreciation, I would like to express my sincere thanks to Dr. Sultan (Director CPM) for his inspiring help and for fully supported the research expense through his project sponsored by King Abdulaziz City for Science & Technology (KACST) through the Science Technology Unit at KFUPM through Project No. 10-ENE-1374 as part of the National Science, Technology and Innovation Plan (NSTIP). I am also indebted to other members of the NSTIP project for their moral support especially Mr J. Adewole. I would like to thank my thesis advisor, Dr. Abdalla Abulkibash, for his inspiring guidance, support and excellent cooperation in supervising this work. His devotion to academic has provided a valuable example to me for my future endeavor that I will always appreciate. I would also like to thank other members of my MS thesis committee, Dr Abdul Rahman Al-Betar and Dr.Amir Al-Ahmed for their immense contribution, suggestions and support throughout the period of this

work.

I will like to give a special thanks to Dr. Belabbes for his suggestions and immense contributions during the course of this work. I also wish to thank all the graduate students and faculty members in Chemistry department. Furthermore, I am highly indebted to the Deanship of Graduate studies through which I got the Kingdom of Saudi Arabia government scholarship for the pursuance of my MS program. The efforts of the following are also appreciated for the spectroscopy characterization of the synthesized catalysts, Dr. A. S Hakeem and Mr. Mazen (XRD), Mr. Qamar (BET Area), Mr. Ateeq (TEM), Mr. Hatim (SEM and EDX) and Mr. Irshad (ICP-MS).

I will like to sincerely appreciate the following individuals for their role in making my MS program a success:- my brothers and sisters- Lekan, Jide, Kayode, Lasun, Damola, Busayo, Labisi, Seun, Taiwo and Shukurat for their prayer and support, my uncles and aunts:- Salman, Tajudeen, Mudathir, Rauf, Mum Aisha, Engr & Hajia Adesokan, Khadijat & Muinat for their support, Salimat, Mrs Fadipe, Mr Tijani J.O, Dr. L. Adams, Uztaz H.Thanni, Mrs A. Agbo, Dr. L. Babalola, Dr. Y. Balarabe & Mr Lawal for their encouragements, support and prayers. Also, I am grateful to all my friends both at home & abroad most especially:- M.Hussain, A.S. Ganiyu, Akinpelu A., Popoola S., Peter A., Sikiru S. & K. Ekuntakoro for their moral and financial support.

This acknowledgement will not be complete without expressing special gratitude to the entire Nigeria community of KFUPM, the M M Y and the Glowing Star Club of Nigeria members for their support at all times. Finally and humbly, I sincerely extend my profound gratitude to all that have been involved to make this work a success.

# TABLE OF CONTENTS

<b>LIST OF TABLES</b>	<b>viii</b>
<b>LIST OF FIGURES</b>	<b>ix</b>
<b>LIST OF SCHEMES</b>	<b>xiii</b>
<b>ABSTRACT (ENGLISH)</b>	<b>xiv</b>
<b>ABSTRACT (ARABIC)</b>	<b>xvi</b>
<b>CHAPTER 1 INTRODUCTION</b>	<b>1</b>
1.1 GENERAL INTRODUCTION . . . . .	1
1.2 General Classification of Fuel Cells . . . . .	2
1.2.1 The Proton Exchange Membrane Fuel Cell (PEMFC) . . . . .	4
1.2.2 Solid Oxide Fuel Cell (SOFC) . . . . .	4
1.2.3 Molten Carbonate Fuel Cell (MCFC) . . . . .	4
1.2.4 Phosphoric Acid Fuel Cell (PAFC) . . . . .	5
1.2.5 Alkaline Fuel Cell (AFC) . . . . .	5
1.2.6 Direct Methanol Fuel Cell (DMFC) . . . . .	5
1.3 Motivation for Current Work . . . . .	10
1.4 Problem Statement . . . . .	11
1.5 Research Objectives . . . . .	13
<b>CHAPTER 2 LITERATURE REVIEW</b>	<b>14</b>
2.1 The Development of Non-Precious Metal Catalysts . . . . .	14

2.2	Carbon Nanotubes . . . . .	28
<b>CHAPTER 3 EXPERIMENTAL</b>		<b>31</b>
3.1	Materials . . . . .	31
3.2	Electrocatalysts Synthesis . . . . .	32
3.3	CNTs Purification and Functionalization . . . . .	32
3.4	Synthesis Procedure . . . . .	36
3.4.1	Sequential Wet Impregnation Method . . . . .	36
3.4.2	Heat Treatment . . . . .	37
3.5	Electrocatalytic activity measurements . . . . .	41
3.5.1	Electrode and Ink Preparation . . . . .	41
<b>CHAPTER 4 RESULTS AND DISCUSSION</b>		<b>45</b>
4.1	Characterization of the highly dispersed Ni-based catalysts . . . . .	45
4.2	Physical Characterization of the Ni-Cu/MWCNTs Catalyst . . . . .	45
4.2.1	X-Ray Diffraction (XRD) Analysis . . . . .	46
4.2.2	FE-SEM Analysis . . . . .	48
4.2.3	Elemental Analysis . . . . .	50
4.2.4	FE-TEM Analysis . . . . .	55
4.2.5	BET Analysis of MWCNTs . . . . .	57
4.3	Cyclic Voltammogram in $N_2$ saturated solution . . . . .	58
4.3.1	Effect of Ni-Cu/MWCNTs Alloy Catalyst Loading . . . . .	61
4.3.2	Ni-Cu/MWCNTs Alloy Catalyst Durability . . . . .	63
4.4	Physical Characterization of Ni-Cu-Mo/MWCNTs Alloy Catalyst . . . .	67
4.4.1	X-Ray Diffraction (XRD) Analysis . . . . .	67
4.4.2	FE-SEM Analysis . . . . .	69
4.4.3	Elemental Analysis . . . . .	71
4.4.4	FE-TEM Analysis . . . . .	75
4.5	Cyclic Voltammogram in $N_2$ saturated solution . . . . .	77
4.5.1	Effect of Ni-Cu-Mo/MWCNTs Alloy Catalyst Loading . . . . .	80
4.5.2	Ni-Cu-Mo/MWCNTs Alloy Catalyst Durability . . . . .	82

4.6	Physical Characterization of Ni-Cu-W/MWCNTs Alloy Catalyst . . . .	86
4.6.1	X-Ray Diffraction (XRD) Analysis . . . . .	86
4.6.2	FE-SEM Analysis . . . . .	88
4.6.3	Elemental Analysis . . . . .	90
4.6.4	FE-TEM Analysis . . . . .	94
4.7	Cyclic Voltammogram in $N_2$ saturated solution . . . . .	96
4.7.1	Effect of Ni-Cu-W/MWCNTs Alloy Catalyst Loading . . . . .	99
4.7.2	Ni-Cu-W/MWCNTs Alloy Catalyst Durability . . . . .	101
<b>CHAPTER 5 CONCLUSION AND RECOMMENDATIONS</b>		<b>105</b>
<b>REFERENCES</b>		<b>107</b>
<b>VITAE</b>		<b>115</b>

# LIST OF TABLES

4.1	EDX Table showing percentage composition of Ni-Cu/MWCNTs alloy catalyst at 900°C . . . . .	53
4.2	EDX Table showing percentage composition of Ni-Cu/MWCNTs alloy catalyst at 1100°C . . . . .	53
4.3	Summary of the average percent by weight of the elements in each alloy catalyst composite . . . . .	53
4.4	BET Analysis table showing the BET surface area, pore volume and pore size of MWCNTs . . . . .	57
4.5	EDX Table showing percentage composition of Ni-Cu-Mo/MWCNTs alloy catalyst at 900°C . . . . .	73
4.6	EDX Table showing percentage composition of Ni-Cu-Mo/MWCNTs alloy catalyst at 1100°C . . . . .	73
4.7	Summary of the average percent by weight of the elements in each alloy catalyst composite . . . . .	73
4.8	EDX Table showing percentage composition of Ni-Cu-W/MWCNTs alloy catalyst at 900°C . . . . .	92
4.9	EDX Table showing percentage composition of Ni-Cu-W/MWCNTs alloy catalyst at 1100°C . . . . .	92
4.10	Summary of the average percent by weight of the elements in each alloy catalyst composite . . . . .	92

# LIST OF FIGURES

2.1	Cyclic voltammograms of C/Ni electrode in 1.0 M KOH + 0.5 M MeOH at a scan rate of 50 mV/s . . . . .	17
2.2	Cyclic voltammograms of NiP/C catalyst in 0.1 M KOH solution in absence and in presence of 0.5 M methanol at 10 mV/s in the potential range from 0 to +1200 mV (MMO) . . . . .	20
2.3	Cyclic voltammograms of the (a) Ni@Pd/MWCNTs, (b) PdNi/MWCNTs, and (c) Pd/MWCNTs catalysts modified electrodes in 0.5 M NaOH +1.0 M CH <sub>3</sub> OH at a scan rate of 50 mV/s.) . . .	23
2.4	Voltammograms for (100-x)% Pd-x% Ni (x = 0, 1, 2, 5, 10 and 20) electrodes in 1 M KOH + 1 M CH <sub>3</sub> OH at scan rate of 50mVs <sup>-1</sup> .) . . . .	25
2.5	Cyclic voltammograms of a NiO/CNT in 0.5 M methanol +1 M KOH solution at a scan rate of 50 mV/s. . . . .	26
2.6	Different Types of CNTs . . . . .	29
3.1	High Temperature Vacuum tube furnace used for the heat treatment of the synthesized catalysts . . . . .	38
3.2	A laboratory set-up for electrochemical measurement . . . . .	42
3.3	A laboratory set-up for electrochemical measurement (catalyst stability) . . . . .	42
4.1	X-ray diffraction (XRD) patterns of Ni-Cu/MWCNTs alloy catalyst at 900°C (a) and 1100°C (b) . . . . .	47
4.2	FE-SEM micrographs of Ni-Cu/MWCNTs alloy catalyst at 900°C (a) and 1100°C (b) . . . . .	49



4.3	EDX Spectrum of Ni-Cu/MWCNTs alloy catalyst at 900°C (a) and 1100°C (b) . . . . .	52
4.4	Elemental Mapping of Ni-Cu/MWCNTs alloy catalyst at 900°C (a) and 1100°C (b) . . . . .	54
4.5	HR-TEM micrographs of Ni-Cu/MWCNTs alloy catalyst at 900°C (a) and 1100°C (b) . . . . .	56
4.6	Cyclic voltammograms of Ni-Cu/MWCNTs electrode formulations at 700°C (a), 900°C (b) and 1100°C (c) in 0.5 M $CH_3OH$ + 0.1 M $KOH$ at a scan rate of 20mV/s . . . . .	59
4.7	Cyclic voltammograms of Ni-Cu/MWCNTs electrode at 900°C (a) and 1100°C (b) in 0.5 M $CH_3OH$ + 0.1 M $KOH$ at a scan rate of 20mV/s . . . . .	60
4.8	Cyclic voltammograms of Ni-Cu/MWCNTs catalyst loading at 900°C (a) and 1100°C (b) in 0.5 M $CH_3OH$ + 0.1 M $KOH$ at a scan rate of 20mV/s . . . . .	62
4.9	Stability Test for Ni-Cu/MWCNTs Cyclic Voltammograms in $N_2$ saturated 0.5 M $CH_3OH$ + 0.1 M $KOH$ . . . . .	64
4.10	Chronoamperometry collected for 10 min at 0.650 V for Ni-Cu/MWCNTs alloy catalyst at 900°C (a) and 1100°C (b) in 0.5 M $CH_3OH$ + 0.1 M $KOH$ . . . . .	66
4.11	X-ray diffraction (XRD) patterns of Ni-Cu-Mo/MWCNTs alloy catalyst at 900°C (a) and 1100°C (b) . . . . .	68
4.12	SEM micrographs of Ni-Cu-Mo/MWCNTs alloy catalyst at 900°C (a) and 1100°C (b) . . . . .	70
4.13	EDX Spectrum of Ni-Cu-Mo/MWCNTs alloy catalyst at 900°C (a) and 1100°C (b) . . . . .	72
4.14	Elemental Mapping of Ni-Cu-Mo/MWCNTs alloy catalyst at 900°C (a) and 1100°C (b) . . . . .	74
4.15	HRTEM micrographs of Ni-Cu-Mo/MWCNTs alloy catalyst at 900°C (a) and 1100°C (b) . . . . .	76

4.16	Cyclic voltammograms of Ni-Cu-Mo/MWCNTs electrode formulations at 700 °C (a), 900 °C (b) and 1100 °C (c) in 0.5 M $CH_3OH$ + 0.1 M $KOH$ at a scan rate of 20mV/s . . . . .	78
4.17	Cyclic voltammograms of Ni-Cu-Mo/MWCNTs electrode at 900 °C (a) and 1100 °C (b) in 0.5 M $CH_3OH$ + 0.1 M $KOH$ at a scan rate of 20mV/s . . . . .	79
4.18	Cyclic voltammograms of Ni-Cu-Mo/MWCNTs catalyst loading at 900 °C (a) and 1100 °C (b) in 0.5 M $CH_3OH$ + 0.1 M $KOH$ at a scan rate of 20mV/s . . . . .	81
4.19	Stability Test for Ni-Cu-Mo/MWCNTs Cyclic Voltammograms in $N_2$ saturated 0.5 M $CH_3OH$ + 0.1 M $KOH$ . . . . .	83
4.20	Chronoamperometry collected for 10 min at 0.650 V for Ni-Cu-Mo/MWCNTs alloy catalyst at 900 °C (a) and 1100 °C (b) in 0.5 M $CH_3OH$ + 0.1 M $KOH$ . . . . .	85
4.21	X-ray diffraction (XRD) patterns of Ni-Cu-W/MWCNTs alloy catalyst at 900 °C (a) and 1100 °C (b) . . . . .	87
4.22	SEM micrographs of Ni-Cu-W/MWCNTs alloy catalyst at 900 °C (a) and 1100 °C (b) . . . . .	89
4.23	EDX Spectrum of Ni-Cu-W/MWCNTs alloy catalyst at 900 °C (a) and 1100 °C (b) . . . . .	91
4.24	Elemental Mapping of Ni-Cu-W/MWCNTs alloy catalyst at 900 °C (a) and 1100 °C (b) . . . . .	93
4.25	HRTEM micrographs of Ni-Cu-W/MWCNTs alloy catalyst at 900 °C (a) and 1100 °C (b) . . . . .	95
4.26	Cyclic voltammograms of Ni-Cu-W/MWCNTs electrode formulations at 700 °C (a), 900 °C (b) and 1100 °C (c) in 0.5 M $CH_3OH$ + 0.1 M $KOH$ at a scan rate of 20mV/s . . . . .	97
4.27	Cyclic voltammograms of Ni-Cu-W/MWCNTs electrode at 900 °C (a) and 1100 °C (b) in 0.5 M $CH_3OH$ + 0.1 M $KOH$ at a scan rate of 20mV/s . . . . .	98

4.28	Cyclic voltammograms of Ni-Cu-W/MWCNTs catalyst loading at 900°C (a) and 1100°C (b) in 0.5 M $CH_3OH$ + 0.1 M KOH at a scan rate of 20mV/s . . . . .	100
4.29	Stability Test for Ni-Cu-W/MWCNTs Cyclic Voltammograms in $N_2$ saturated 0.5 M $CH_3OH$ + 0.1 M KOH . . . . .	102
4.30	Chronoamperometry collected for 10 min at 0.650 V for Ni-Cu-W/MWCNTs alloy catalyst at 900°C (a) and 1100°C (b) in 0.5 M $CH_3OH$ + 0.1 M KOH . . . . .	104

# LIST OF SCHEMES

1.1	Schematic diagram of a typical fuel cell . . . . .	3
1.2	Schematic diagram of direct methanol alkaline fuel cell. . . . .	8
2.1	Electro-Deposition of Pt and Ni nanoparticles on MWCNTs through a three-step process . . . . .	19
2.2	The novel method for the synthesis of Ni@Pd electrocatalysts on MWCNTs . . . . .	22
3.1	Functionalization of CNTs . . . . .	34
3.2	Schematic procedure for functionalization of CNTs . . . . .	35
3.3	Sequential Wet Method + Freeze Drying Procedure for Metal Sup- ported Catalyst Synthesis . . . . .	39

# THESIS ABSTRACT

**NAME:** OLANREWAJU SULEIMAN OLAKUNLE

**TITLE OF STUDY:** SYNTHESIS AND CHARACTERIZATION OF HIGHLY  
DISPERSED NICKEL-BASED CATALYSTS FOR ALKA-  
LINE DIRECT METHANOL FUEL CELLS

**MAJOR FIELD:** CHEMISTRY

**DATE OF DEGREE:** December 2014

*Methanol oxidation reaction (MOR) is of great technological interest because of its potential application to direct methanol fuel cells (DMFCs), which show great potential as high-efficiency, low-emission future power source. Platinum is one of the best catalysts for methanol oxidation reaction (MOR), but apart from its high cost and limited abundance, it is generally recognized that pure Pt is prone to carbon oxide (CO) poisoning, which is an intermediate in the methanol oxidation reaction (MOR). However, the overall objective of the work is to develop potentially low cost and efficient platinum-free anode catalysts to at least overcome the issue of high cost of Pt as well as the use of alkaline medium to hasten the kinetics of methanol oxidation reaction. As far as development of Pt-free anode catalysts are concerned, the major contribution in this work*

*focused on incorporating varying composition of Ni metal and co-catalyst metals (Cu, W, and Mo) on carbon support especially multi-walled carbon nanotubes (MWCNTs). The approach is based on impregnation of a metal salt used as precursor with another metal salt and added drop wise to the functionalized MWCNTs slurry. The synthesis conditions were carefully tailored to reduce particle agglomeration, which after heat treatment generated highly active sites Ni-Mx or Ni-Mx-My/MWCNTs for methanol oxidation reaction. The heat treatment is important in order to tune the physicochemical properties of carbon support (MWCNTs) to form the said highly dispersed Ni-based electro-catalysts. The obtained electro-catalysts were characterized by using electrochemical techniques Chronoamperometry (CA), potential cycling and Cyclic voltammetry (CV) for their activities towards MOR, durabilities, stabilities and also by spectroscopic techniques to investigate their morphological structures and compositions using TEM (Transmission Electron Microscopy), XRD (X-ray Diffraction technique), Elemental mapping, ICP-MS (Inductively Coupled Plasma-Mass Spectroscopy), FE-SEM (High-end Field Emission Scanning Electron Microscopy), EDX (Energy-dispersive X-ray spectroscopy).*

الإسم : سليمان اولاكونل اولانريواجو

العنوان : تصنيع وتحليل محفزات النيكل المتناثرة جيداً لخلايا الوقود القاعدية المباشرة

الدرجة: ماجستير في العلوم

التخصص: الكيمياء

تاريخ منح الدرجة: ديسمبر 2014

### ملخص الرسالة

تعتبر خلايا وقود الميثانول المباشرة من التقنيات الواعدة حيث يمكن استخدامها كمصدر عالي الكفاءة لتوليد الطاقة ويتميز هذا المصدر بقلّة النواتج المنيعة ويعتبر هذا المصدر صديقاً للبيئة. وتعتمد هذه الخلايا على أكسدة الميثانول باستخدام البلاتين كقطب لعملية الأكسدة وبالرغم من أن البلاتين يعتبر واحداً من أفضل المحفزات المستخدمة في تفاعلات أكسدة الميثانول إلا أنه وبغض النظر عن تكلفته العالية ووفرتة المحدودة إلا أنه يكون عرضة للتسمم بغاز أول أكسيد الكربون الناتج من تفاعلات أكسدة الميثانول.

يهدف هذا البحث إلى تطوير محفزات أنودية فاعلة وقليلة التكلفة ويمكن استخدامها في وسط قاعدي يعمل على زيادة سرعة تفاعل أكسدة الميثانول. وتعتمد فكرة هذا البحث على دمج تركيبات مختلفة من معدن النيكل مع محفزات مشاركة من معادن النحاس والتنجستون والمولبدنوم تركز على دعامة مكونة من أنابيب الكربون النانوية متعددة الجدران. ويتم خلط ملح النيكل مع ملح من معدن آخر ويضاف الخليط قطرة قطرة إلى أنابيب الكربون النانوية متعددة الجدران. وتم الحصول على الظروف المثلى لتحضير هذا الحفاز بحيث لا يتم تكتل الجسيمات، والتي بعد معالجتها حرارياً تولد مواقع نشطة جداً مكونة إما من النيكل والمعدن الأول أو من النيكل والمعدنين و أنابيب الكربون النانوية متعددة الجدران والتي أثبتت فاعليتها في أكسدة الميثانول. ووجد بأن المعالجة الحرارية تعتبر مهمة وذلك لضبط الخواص الفيزيوكيميائية لدعامة أنابيب الكربون النانوية متعددة الجدران لكي يتم توزيع الخواص الكهربائية لهذا النوع من الحفازات. ولقد تم تحضير ستة أنواع من هذه الحفازات وأثبتت فاعليتها في أكسدة الميثانول. ولقد تم توصيف هذه الحفازات باستخدام التقنيات الكهروكيميائية (مقياسية التيار والزمن والجهد الدوري ومقياسية الفولت الدوري) وذلك لنشاطها تجاه تفاعلات أكسدة الميثانول، ومثابقتها وثباتها وكذلك بالتقنيات الطيفية لفحص تركيبها المورفولوجي ومكوناتها باستخدام مجهر الانتقال الإلكتروني، وحيود الأشعة السينية، وكشف الخرائط للعناصر، وكشف البلازما المقترنة المستحثة مع مطيافية الكتلة، ومجهر المسح الإلكتروني الانبعاث المجالي، ومطيافية الأشعة السينية مشتتة الطاقة.



# **CHAPTER 1**

## **INTRODUCTION**

### **1.1 GENERAL INTRODUCTION**

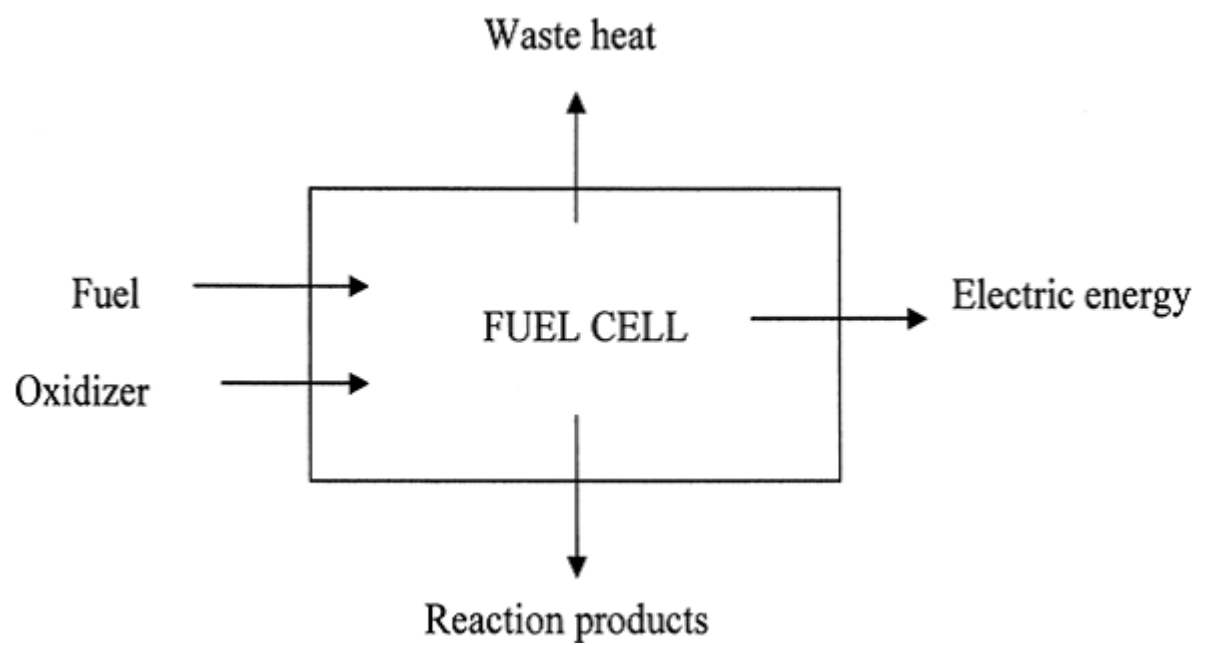
Fuel cells are electrochemical devices that efficiently convert chemical energy from a hydrogen- rich fuel source into electrical energy with exceptionally low emissions and without combustion (combustion-free). They are attractive power sources for both stationary and electric vehicle applications due to their high conversion efficiencies and low pollution. They are becoming well established in a number of markets where they are now recognized as a better technology option than conventional internal combustion engine generators i.e efficient and environmental friendly [1]. In contrast to internal combustion engines, the fuel is not combusted; instead the energy is being released electrocatalytically and makes fuel cells to be highly energy efficient. They produce electricity directly from electrochemical reaction of hydrogen, from hydrogen-rich fuel especially methanol and oxygen from air. Energy conversion by a fuel cell depends largely upon catalytic electrodes, which accomplish electrochemical reaction that con-

vert fuel into electrical energy without involving burning process. They use an external supply of chemical energy and can run continuously, as long as a source of hydrogen especially methanol is supplied together with a source of oxygen (usually air)[2]. Fuel cells are example of devices where surface electrochemistry plays the central role. Thus, surface electrochemistry is the part of chemistry concerns with the interaction of molecules with the surface.

## 1.2 General Classification of Fuel Cells

There are various types of fuel cells which include Proton Exchange Membrane Fuel Cells (PEMFCs), Solid Oxide Fuel Cells (SOFCs), Molten Carbonate Fuel Cells (MCFCs), Phosphoric Acid Fuel Cells (PAFCs), Alkaline Fuel Cells (AFCs) as well as direct methanol fuel cells (DMFCs) which are relatively recent addition to the field of fuel cell technologies. Fuel cells convert the chemical energy arising from reaction between hydrogen ( $H_2$ ) and oxygen ( $O_2$ ) directly into electrical energy, water and heat [3]. The general block diagram of a fuel cell is given in Scheme 1.1

The fuel cells can be classified based on the nature/type of the electrolyte used, apart from direct methanol fuel cells (DMFCs) that use methanol as a fuel or based on their temperature of operation: high, medium and low temperature fuel cells:



Scheme 1.1: Schematic diagram of a typical fuel cell

### **1.2.1 The Proton Exchange Membrane Fuel Cell (PEMFC)**

The Proton Exchange Membrane Fuel Cell (PEMFC) is a class of device used for the conversion of chemical energy into electrical energy and uses a water-based, acidic polymer membrane as its electrolyte, with platinum-based-electrodes. It is the most promising and considered as a suitable candidate for electric vehicles as well as in stationary applications due to its low operating temperature ( $<100^{\circ}\text{C}$ ). PEMFC is also known as Polymer Electrolyte Membrane Fuel Cell.

### **1.2.2 Solid Oxide Fuel Cell (SOFC)**

The Solid Oxide Fuel Cell (SOFC) has emerged as a promising technology for efficient electrochemical energy conversion. It contains four basic components: anode, electrolyte, and cathode as well as interconnect. The electrolyte commonly used for many years is solid ceramic electrolyte (yttria-stabilized zirconia (YSZ)) and a Ni/YSZ has been used as an anode, where the fuel is electro-catalytically oxidized at the three-phase boundary of the electrode. SOFC operates at a very high temperatures (in the range of  $800^{\circ}\text{C}$  to  $1000^{\circ}\text{C}$ ). It is commonly used in small and large stationary power generations.

### **1.2.3 Molten Carbonate Fuel Cell (MCFC)**

This type of fuel cell uses a molten carbonate salt (such as lithium carbonate, potassium carbonate, or sodium carbonate) suspended in a porous ceramic matrix as an electrolyte and can run on hydrocarbon fuels such as methane. It operates at around  $650^{\circ}\text{C}$  and

runs continuously more efficiently at high operating temperatures. MCFC is mostly used in large stationary power generations.

#### **1.2.4 Phosphoric Acid Fuel Cell (PAFC)**

Phosphoric acid fuel cell (PAFC) uses liquid phosphoric acid in a bonded silicon carbide matrix and a finely dispersed platinum catalyst on carbon which acts as a cathode and anode respectively. It is quite resistant to poisoning by carbon monoxide and operates at moderate temperatures around 180°C. Its electrical efficiency is relatively low, but if heat is used, the overall efficiency can reach 80%. It is mostly applied in stationary power generation and also in large vehicles, such as buses.

#### **1.2.5 Alkaline Fuel Cell (AFC)**

Alkaline Fuel Cell (AFC) was one of the first fuel cells technologies invented in 1839 by Sir William Robert Grove. This uses alkaline solution such as potassium hydroxide (KOH) in water as an electrolyte and nickel catalyst is commonly used. The typical operating temperature in modern AFCs is around 70°C. It is generally fueled with pure hydrogen. AFC is mostly used in NASA shuttles throughout the space programme.

#### **1.2.6 Direct Methanol Fuel Cell (DMFC)**

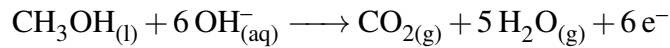
The Direct Methanol Fuel Cell (DMFC) is a relatively recent addition to the field of fuel cell technologies. DMFC is similar to PEMFC because it also uses polymer membrane as an electrolyte. The anode catalyst (usually platinum-ruthenium) in DMFC is able

to draw the hydrogen gas generated from liquid methanol and then no need for a fuel reformer, thus the system can be made much simpler. Methanol has several advantages as a fuel because it is cheap and renewable. In addition, methanol has a relatively high energy density, can be easily transported and stored. DMFC operates at a lower temperature range from 60°C to 130°C. They do not require any fuel processor, thus they can be operated at room temperature. Direct methanol fuel cells (DMFCs) are considered as promising candidates for applications in portable power sources, electric vehicles and transport applications. Also, it tends to be used in applications with modest power requirements, such as mobile electronic devices or chargers and portable power packs.

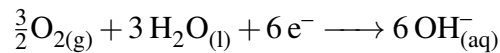
DMFC can be operated both in acidic (protonic) and alkaline media;

1. Acidic (protonic) electrolyte based DMFC is directly fed with a methanol/water mixture at the anode. Methanol is directly oxidized to carbon dioxide with the possible formation of organic compounds such as formaldehyde or formic acid is not excluded. The formation of such organic molecules decreases the amount of fuel used which makes the kinetics to be slow. Also, there is methanol crossover from the anode fuel to the cathode and relatively low activity of methanol oxidation electrocatalysts.
2. Alkaline (lower methanol permeability) electrolyte based DMFC is more favored than protonic DMFC because there is reduction in methanol cross-over and the kinetic becomes more facile for ORR and MOR. The drawbacks (i.e carbonate formation and need to frequently regenerate the electrolyte) associated with con-

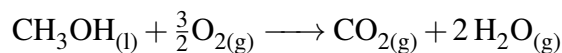
ventional aqueous KOH electrolyte fuel cells have been overcome by the development of new membranes such as alkaline anion exchange membranes (AAEMs) [4, 5]. Moreover, non-precious metals such as Ni can be used as a base metal because they are chemically more stable in alkaline media and no poisoning of the intermediates as in case of Pt electrocatalysts in acidic medium. Furthermore, catalysts corrosion and membrane degradation are significantly mitigated due to the high pH [4]. Thus, a wider number of catalyst formulations can be investigated for methanol oxidation than for proton conducting electrolytes. In alkaline DMFCs, methanol is oxidized at the anode as shown below;



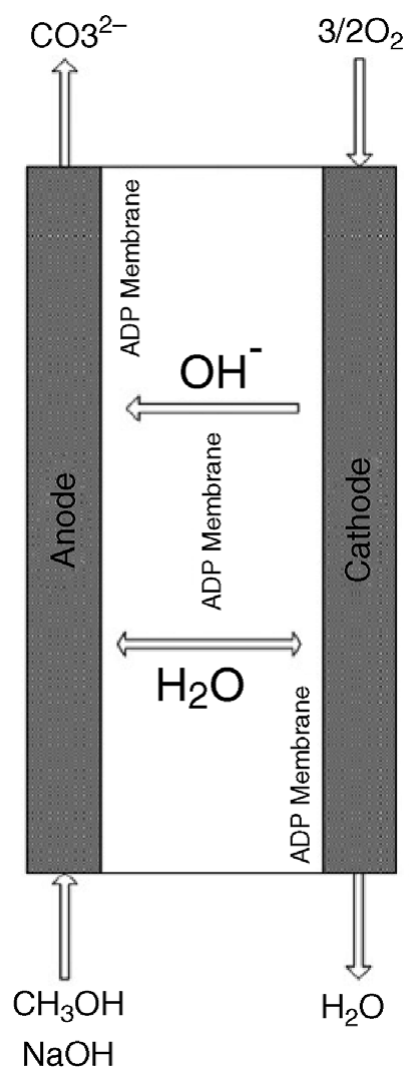
It is possible that a methanol molecule and a water molecule move to the surface of the electrode, where they react in a single step and pass six electrons to the electrode. However, the actual process is more complicated than this because methanol and water can react with the surface to give intermediate molecules that are adsorbed on the surface. The  $\text{OH}^-$  ions necessary for ions conduction are formed at the cathode by the water added to humidify the oxidant and these ions migrate to the anode thereby reducing methanol crossover by the electro-osmotic drag [4]. Scheme 1.2 shows the schematic diagram of the alkaline DMFC. The oxygen reduction reaction (ORR) takes place at the cathode as shown below;



The overall reaction will be as follow;







Scheme 1.2: Schematic diagram of direct methanol alkaline fuel cell.

Methanol oxidation reaction (MOR) is of great technological interest because of its potential application to direct methanol fuel cells (DMFCs) [6], which show great potential as high-efficiency, low-emission future power source [7]. Platinum is one of the best catalysts for methanol oxidation reaction (MOR), but apart from its high cost and limited abundance, it has been recognized that pure Pt is prone to carbon monoxide (CO) poisoning at moderate temperatures. Carbon monoxide is an intermediate in the oxidation reaction of methanol [8, 9]. In order to obtain high efficiency in DMFC, an anodic MOR catalyst that is not prone to CO poisoning is required. Thus, the need for suitable alternatives to precious metal catalysts (i.e. Pt, Pd) that are comprised of cheap and earth-abundant elements. In addition to that, the metals must possess good catalytic activity and selectivity. Considering the importance of nickel-based materials as suitable catalysts for the oxidation of alcohols, in addition to the spatial properties of CNTs, the target of the present work was to apply MWCNTs as a catalyst support to improve the electro-catalytic activity of glassy carbon/nickel based electrode in alkaline solution [10]. MOR in alkaline medium involves the formation of higher valence Ni-oxide, which acts as a chemical oxidizing agent. The presence of Ni-oxide in the electro-catalyst provides an oxygen source for CO oxidation at lower potentials [11]. As a result of optimizing the synthesis methods and exploring various transition-metals, Ni-based catalyst was found to be a promising alternative to platinum. It is generally accepted that MOR activity and durability are largely determined by the type of the transition metals in the electro-catalyst, the type of carbon support (e.g CNTs) used, the synthesis conditions and the medium used e.g alkaline solution [12]. Furthermore,

several experimental studies of the Ni-alloy anode catalysts have shown the advantages of the alloying elements i.e co-catalysts (e.g W, Mo, Cu Fe and Sn) on the performance of the fuel cell [13]-[18]. Moreover, it was reported that utilizing multi-walled carbon nanotubes (MWCNTs) and their composites as Ni-based catalysts support produced by the pyrolysis of the Ni-Mx/MWCNTs or Ni-Mx-My/MWCNTs have catalyzed efficient MOR process. As a result, a much higher electro-catalytic activity, lower overpotential, high oxidative stability, good electronic conductivity, high surface area and better long-term operation stability than that of Pt-based electrodes in alkaline electrolytes have been noted [19]-[21].

### **1.3 Motivation for Current Work**

The active metals like (Ni, Cu, Mo & W) when supported on a support of high surface area such as multi-walled carbon nanotubes(MWCNTs) may increase the current flux density and lower the overpotential needed for the oxidation of methanol which is considered as a surface phenomenon. Thus, the role of Cu, W or Mo in the complex nano-composite catalyst used for the electrocatalysis of methanol in alkaline medium is a synergic effect (co-catalyst) which may lead to increase in the activity of the catalyst. It was therefore planned to prepare bi/tri- nanocomposites of Ni and Cu, W or Mo of varied compositions with an aim to optimize the percentage of Cu, W or Mo in the composite for producing the highest electrocatalytic effect and then increase its electrocatalytic activity further through addition of an amount of carbon nanotube. These supported non-precious metals electrocatalysts can be conveniently used in pro-

ton exchange membrane fuel cells (PEMFCs) especially the direct methanol fuel cells (DMFCs) types.

This work focuses on incorporating varying composition of Ni metal and co-catalyst metals (Cu, W, and Mo) on carbon support especially multi-walled carbon nanotubes (MWCNTs) because of their promotional effect on catalytic activity and their enhancement to the mass transfer process at the electrodes. In addition, MWCNTs have better resistance to electrochemical corrosion than carbon black (CB). This is due to the ability of functionalized MWCNTs to complex with Ni precursors ( $Ni(NO_3)_2 \cdot 6H_2O$ )/co-catalysts and generate under heat treatment highly active sites which is able to tune the physico-chemical properties of multi-walled carbon nanotube support. As a result, the formation of the highly dispersed Ni- Nano catalysts which are considered as electro-catalysts for methanol oxidation reaction.

These synthesized alloy catalysts were characterized for their activities, stabilities, compositions and morphologies in order to get indepth understanding of their catalytic behavior as non-precious metal (Pt-free) based anode catalysts. The following techniques were applied; spectroscopic techniques (ICP-MS, TEM, XRD, SEM and EDX), electrochemical techniques (Chronoamperometry (CA) and Cyclic voltammetry (CV)).

## 1.4 Problem Statement

Fuel cells are well established efficient power generation sources, i.e high efficiency and low emission. They can make a significant contribution to the environment protec-

tion as well as sources of sustainable energy in the nearest future. In a direct methanol fuel cell especially one with acid as electrolyte, methanol oxidation reaction (MOR) is much slower and there is also the methanol crossover from the anode. This makes MOR one of the critical factors limiting the performance of the direct methanol fuel cells (DMFCs). At present, platinum-based materials are the most widely used as electrocatalysts for MOR. However, the problems of durability, scarcity, and high cost of Pt still hamper the commercial applications of the direct methanol fuel cells significantly. The synthesis method as well as the support material and synergic metals (co-catalysts) have been identified as major determining factors in order to develop non-precious metals (NPM) nano-catalysts with desirable properties which are known to be Pt-based materials disadvantages. During the course of this work, efforts were directed towards ensuring that the problems of some common synthesis methods are avoided such as sintering of catalyst particles (i.e agglomeration). For the first time the functionalized multi-walled carbon nanotubes (O-MWCNTs) which are easily dispersed in water were used as supports for this application. A large number of carboxyl groups are formed on their surfaces, the fact that gives them polar characteristic. This helps to overcome low catalytic activity and efficiency towards MOR.

The base metal (Ni) in conjunction with synergic metals (co-catalysts) were employed in the development of non-precious metal (NPM) nano- catalysts which help to reduce poor selectivity (active towards ORR during crossover of oxygen) as well as to enhance the chemical and electrochemical stability in alkaline medium (lower methanol permeability electrolytes) and also to increase the catalytic activity.

## 1.5 Research Objectives

The main objective of this work is to develop new highly dispersed non-precious metals catalysts that can be used for methanol oxidation reaction (MOR) in alkaline medium.

In addition, the following can also be considered as objectives of the work;

1. To develop low cost, active, and durable catalyst systems for DMFC anode reaction (Methanol oxidation reaction, MOR).
2. To develop catalysts based on nickel alloys, such as Ni-Mx/MWCNT/ Ni-Mx-My/MWCNT (Mx=Cu, My= W/Mo) for anodic methanol oxidation reaction in alkaline fuel cells.
3. To enhance active sites (dispersion of catalyst metals, high surface area) for MOR activity.
4. To understand the electrochemical properties of developed nano-catalysts.
5. To characterize in depth the synthesized nano-catalyst using ICP-MS, XRD, SEM-EDX and TEM to provide information about morphology, microstructure, composition, and surface functionalities in order to highlight the active sites towards MOR.
6. To evaluate the performance of developed nano-catalysts in alkaline medium using three-electrode cell configuration.
7. To obtain a good surface area of functionalized MWCNTs.

## **CHAPTER 2**

# **LITERATURE REVIEW**

### **2.1 The Development of Non-Precious Metal Catalysts**

In the development of low cost and efficient platinum-free catalyst, a change of electrolyte is one of the main issues considered to overcome the problem of slow kinetics of the methanol oxidation reaction (MOR). Also, the high cost associated with platinum based catalysts and methanol crossover have to be considered too. The previous studies showed that non- precious metal (NPM) catalysts based on carbon support for methanol oxidation reaction are promising alternatives to platinum based catalysts in fuel cells due to their low cost and readily availability. However, their low catalytic activity and durability still do not meet the fuel cell requirements for commercialization.

In 1922, Muller first explored methanol electro-oxidation process and later in early 1950s, Kordesch and Marko as well as Pavela started the investigation of the concept of methanol fuel cells. At the same time much research work on the anode and cathode electrocatalysts for such an application was initiated. Then, the search for active anode

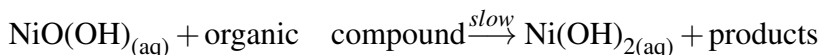


and cathode catalysts mainly regarded nickel or platinum for the MOR and silver for the oxygen reduction process [22].

Cathro have investigated the Pt-Sn system and also Jansen and Molhuysen, their work were among the pioneering studies carried out on catalysts for methanol oxidation which represented the first attempts to make a screening of bimetallic catalysts using a systematic method. The Pt-Sn and Pt-Ru systems were isolated as the most promising anode formulations and in effect Pt-Sn system was a better catalytic system [23]. Further studies by Watanabe and Motoo in the 1960s showed the large potentialities of the Pt-Ru system especially when Pt and Ru were combined in a solid solution (face centered cubic (fcc) alloy) [24].

The previous work on the anode catalysts for MOR mainly addressed the investigation of the mechanism and the search for new or improved catalyst formulations. One of the first attempts to rationalize the MOR was by Bagotzky and Vassiliev, their work essentially was carried out on pure platinum [25]. These studies served as a basis for the successive formulation of the bifunctional theory for bimetallic catalysts [24]. Also, the successive attempts of Parsons and Vander-Noot [26] and Aramata [27] to further rationalize the mechanisms of MOR by electrochemical studies.

Fleischmann et al. 1971, [28] suggested that the organic species are oxidized by a mechanism involving non-direct electron transfer from the organic compound to the anode which was given by;



According to the above mechanism, in the presence of methanol there is an accumulation of  $Ni(OH)_2$  species and this necessarily evolves towards more stable species and its oxidation is attained at more positive potentials. Van Effen et al. 1979, [19] have found that the oxidation of ethanol in KOH involved the formation of higher valence Ni-oxide, which acts as a chemical oxidizing agent. In the late 1980s and beginning of the 1990s, McNicol et al [29] have observed in their Pt electrocatalysts that the maximum activity was found to be at about  $80\text{ m}^2/\text{g}$  surface area. Also, another group showed that the specific activity increases as a function of particle size [30]. Watanabe et al [31] have discovered that the specific activity for MOR on a carbon supported Pt electrocatalyst does not change for a particle size above 2 nm; thus the mass activity increases as the dispersion of the metal phase is increased [31].

Other studies have shown that it is possible to enhance the mass transport at the electrode and at the same time reduce the ohmic drop. In 1994, Taraszewska et al. [32] have found that glassy carbon/ $Ni(OH)_2$  modified electrode acts as an effective catalyst for the oxidation of methanol. Abdel Rahim et al. 2004, [33] have prepared Ni catalyst by electro-deposition from acidic  $NiSO_4$  solution using potentiostatic and galvanostatic techniques and found that only Ni dispersed on graphite shows good catalytic activity towards methanol oxidation but massive Ni does not. Fig 2.1 shows the cyclic voltammetric behavior of the catalyst (C/Ni) in 1.0 M KOH in the presence of 0.5 M MeOH.

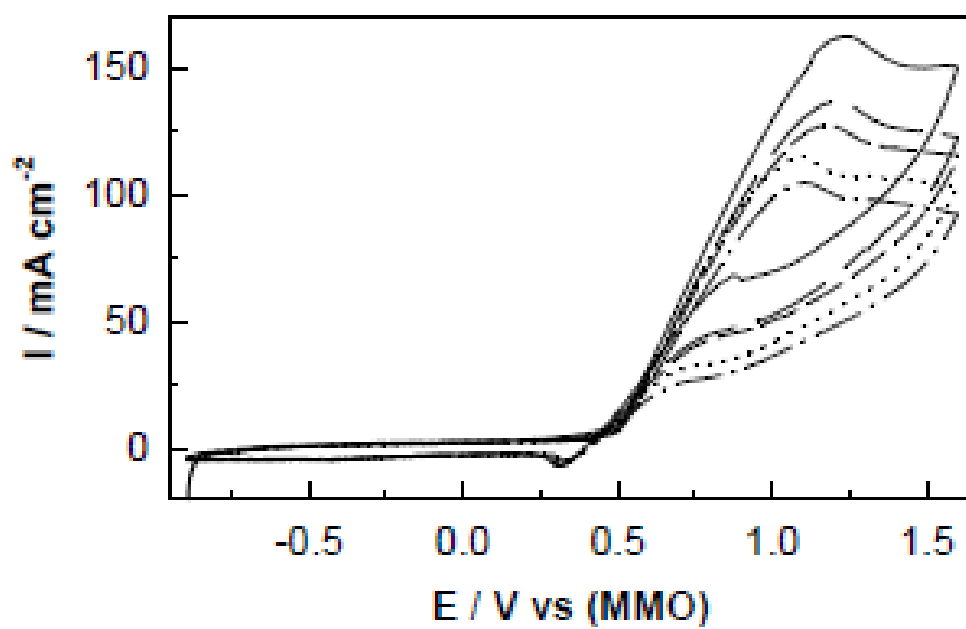
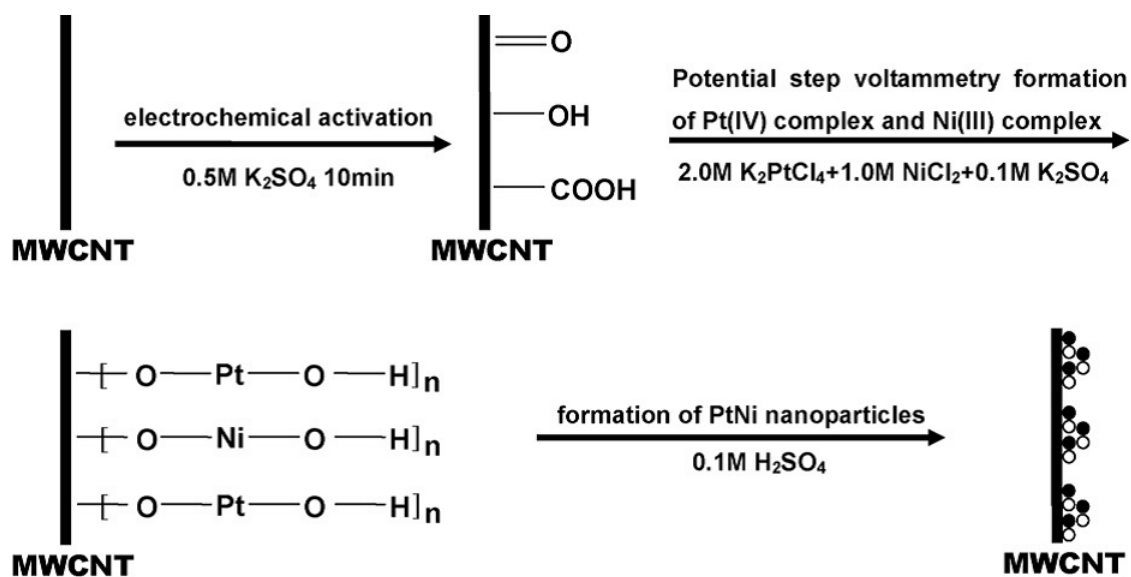


Figure 2.1: Cyclic voltammograms of C/Ni electrode in 1.0 M KOH + 0.5 M MeOH at a scan rate of 50 mV/s

Also in 2004, Mascaro et al. [34] have developed binary NiMo alloys prepared by induced codeposition process. The influence of metallic ion concentration on the voltammetric response was studied at three different ratios. Fan et al. 2007, [35] have prepared Pt-Ni alloy nano-catalysts by a new novel method called electro-deposition on MWCNTs through a three-step process as given in the following scheme 2.1.

Similarly, an excellent MOR activity had been reported by Abdel Hameed and El Khatib 2009, [36] using *NiP* and *NiCuP* supported over commercial carbon electrodes prepared by electroless deposition technique. Fig 2.2 shows the cyclic voltammogram of *NiP/C* catalyst in 0.1 M KOH solution after the addition of 0.5 M methanol at 10 mV/s and they also studied the effect of repeated potential of the catalysts.



Scheme 2.1: Electro-Deposition of Pt and Ni nanoparticles on MWCNTs through a three-step process

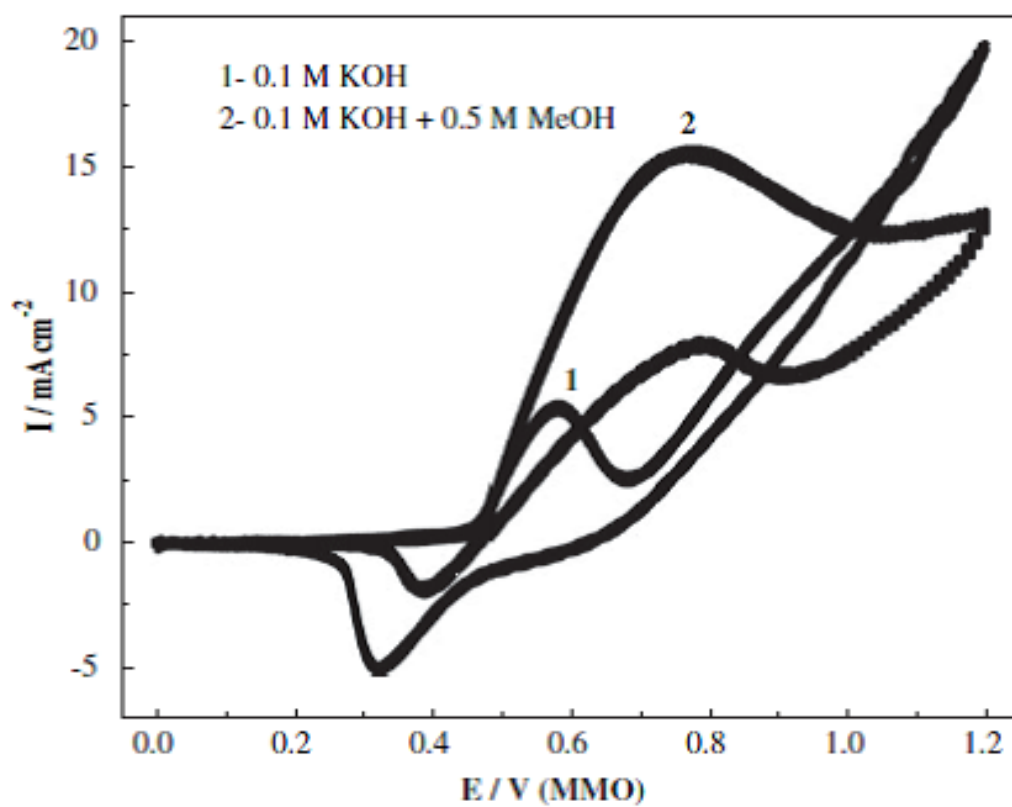
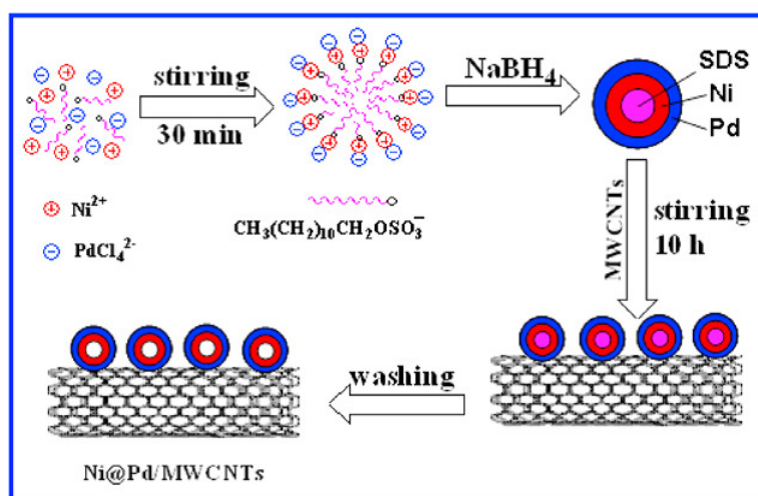


Figure 2.2: Cyclic voltammograms of NiP/C catalyst in 0.1 M KOH solution in absence and in presence of 0.5 M methanol at 10 mV/s in the potential range from 0 to +1200 mV (MMO)

Another family of catalysts had been reported by Zhao et al 2010, [37] where Ni@Pd core shell nanoparticles as a novel anode catalyst for the alkaline DMFC without platinum. The Ni@Pd nanoparticles supported on MWCNTs were prepared by the co-reduction of  $Ni^{2+}$  and  $PdCl_4^{2-}$  in sodium dodecyl sulfate (SDS) as capping and structure-directing agent as given in the scheme 2.2.

The effects of formulations on the catalytic activity of MOR and the stability of the catalysts have been reported. They observed that the adsorption/desorption of hydrogen appeared between  $-1.0$  V and  $-0.7$  V but somewhat more negative potentials on Ni@Pd/MWCNTs than for others and Fig 2.3 shows that Ni@Pd/MWCNTs has high electrochemically active surface area as given below.



Scheme 2.2: The novel method for the synthesis of Ni@Pd electrocatalysts on MWCNTs



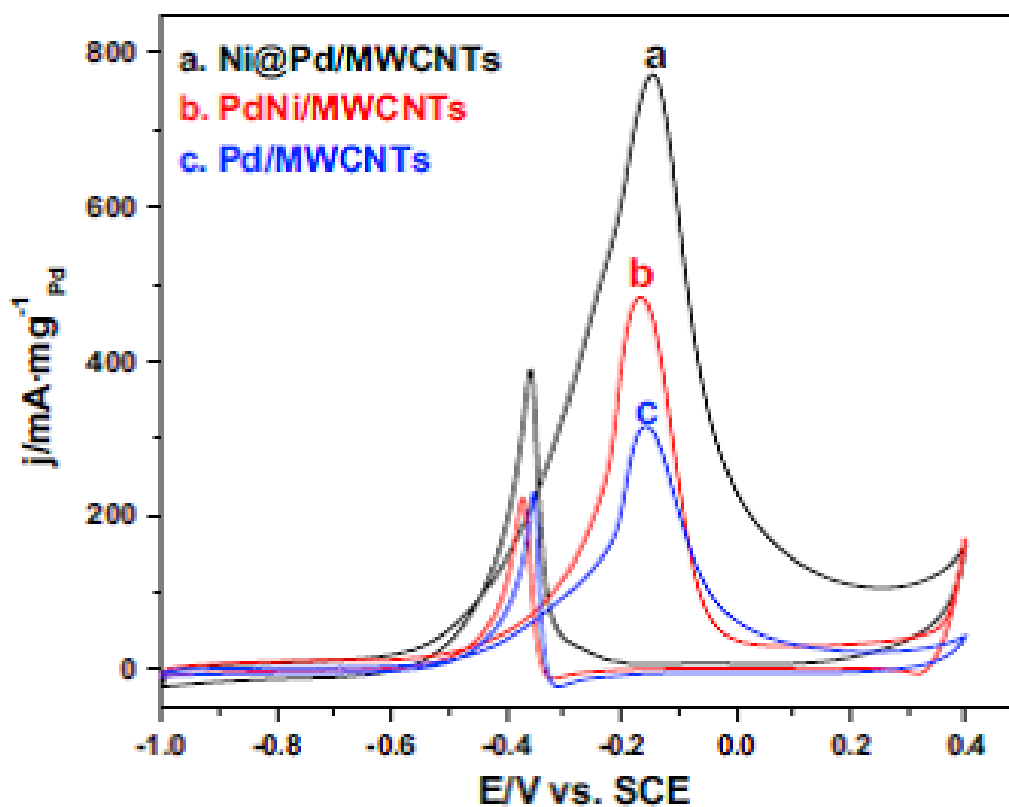


Figure 2.3: Cyclic voltammograms of the (a) Ni@Pd/MWCNTs, (b) PdNi/MWCNTs, and (c) Pd/MWCNTs catalysts modified electrodes in 0.5 M  $\text{NaOH}$  + 1.0 M  $\text{CH}_3\text{OH}$  at a scan rate of 50 mV/s.)

Singh et al. 2010, [38] have synthesized nanostructured Pd-x wt % C ( $x = 0.5, 1, 2$  and 5 and Pd-y wt % MWCNT ( $y = 1, 2$  and 5) using the borohydride reduction method and have investigated the electrocatalysis of methanol oxidation reaction in 1 M KOH at 25 °C. Fig 2.4 shows Voltammograms for (100-x)%Pd-x% Ni( $x = 0, 1, 2, 5, 10$  and 20) electrodes in 1 M KOH + 1 M CH<sub>3</sub>OH at a scan rate of 50 mV/s. Antolini et al. 2010, [39] presented in their work an overview of the use of tungsten-containing materials in fuel cells. They reported that Tungsten-based materials can play different roles in the fuel cell systems. They observed that these materials are the only compounds which can serve as catalysts, co-catalysts, catalyst supports as well as electrolytes in different types of fuels cells. They concluded that tungsten-based materials fulfilled the requirements for the applications as thermally stable carbon-alternative catalyst supports and Nafion®-alternative proton conducting electrolytes in fuel cells operating at an intermediate temperature. In 2012, Qin et al. [40] have prepared hybrid structure NiO/CNT catalyst by atomic layer deposition (ALD) technique. They reported that the NiO/CNT hybrid nanostructures exhibit high performance in the electro-catalytic oxidation of methanol. Fig 2.5 shows the electro-oxidation of methanol in a N<sub>2</sub> -saturated solution of 1 M KOH containing 0.5 M CH<sub>3</sub>OH at a scan rate of 50mVs<sup>-1</sup> and given below;

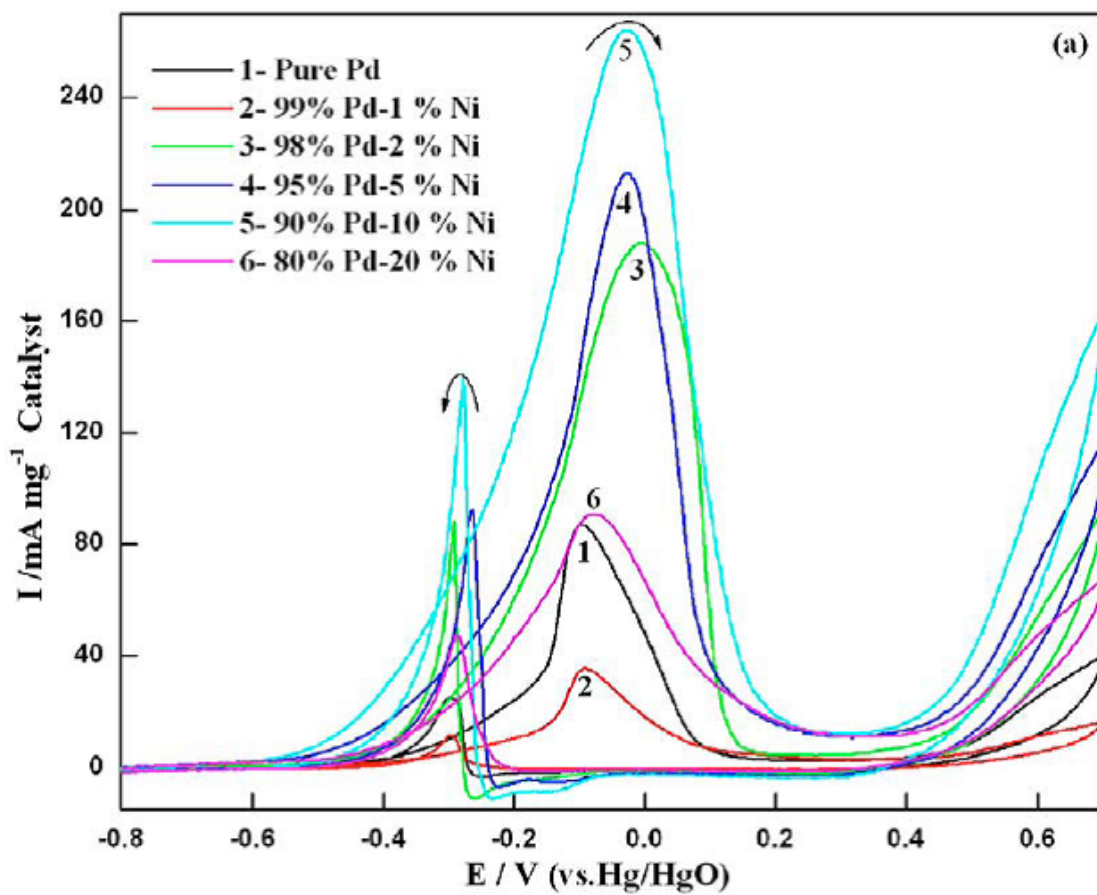


Figure 2.4: Voltammograms for (100-x)% Pd-x% Ni ( $x = 0, 1, 2, 5, 10$  and  $20$ ) electrodes in  $1 \text{ M KOH} + 1 \text{ M CH}_3\text{OH}$  at scan rate of  $50 \text{ mVs}^{-1}$ .)

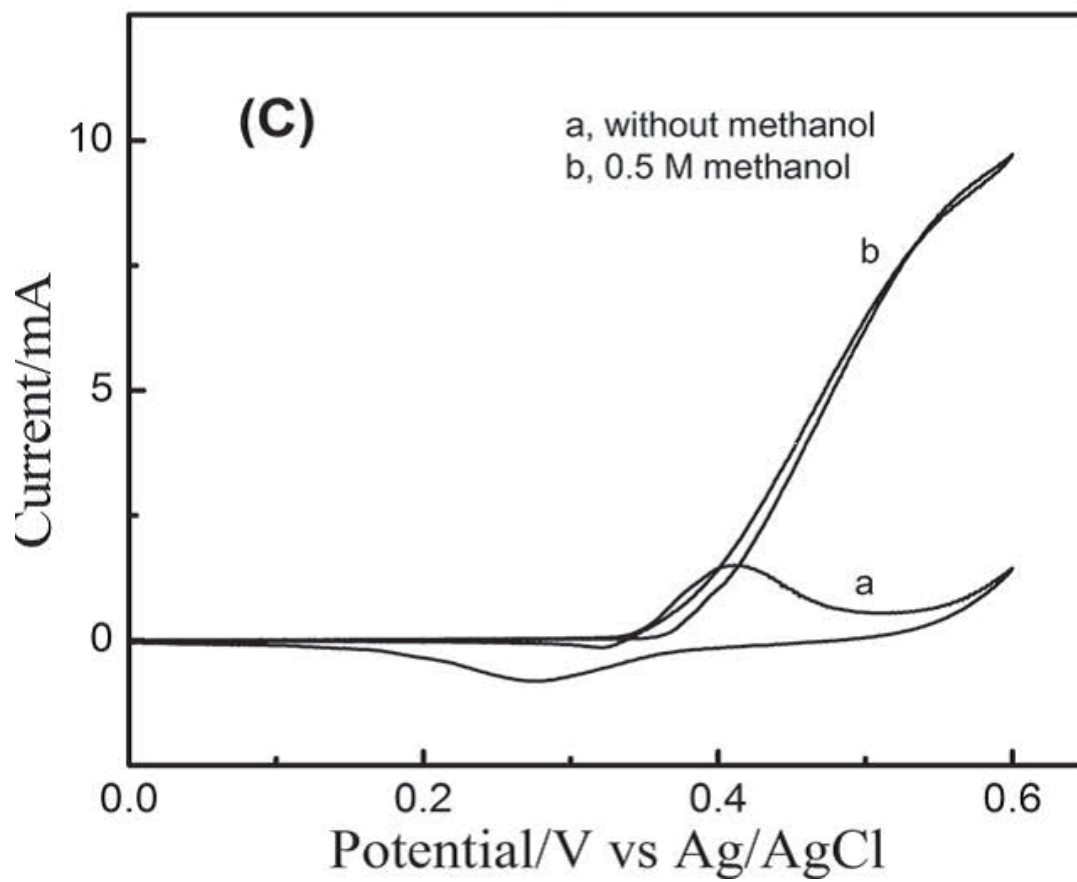


Figure 2.5: Cyclic voltammograms of a NiO/CNT in 0.5 M methanol +1 M KOH solution at a scan rate of 50 mV/s.

Sahin et al. 2013, [41] have prepared Cu-Ni(Zn)-Co catalyst on a copper substrate by using electrodeposition technique. They have reported that the catalytic efficiency of methanol oxidation using cyclic voltammetry techniques. In 2013, El-Khatib et al. [42] have prepared Ni and Pd-Ni nanoparticles catalysts chemically deposited on Vulcan XC-72R carbon black by impregnation method using  $NaBH_4$  as a reducing agent. They have reported that the catalytic efficiency of methanol oxidation using cyclic voltammetry techniques.

Abdel Hameed et al. 2013, [43] have prepared Pd, Ni and PdNi nanoparticles catalysts uniformly dispersed on Vulcan XC-72R carbon black by microwave-irradiation method using  $NaBH_4$  as a reducing agent. They have noted that, the nanocatalysts are properly alloyed and show good catalytic efficiencies for methanol oxidation using cyclic voltammetry techniques. Abdel Hameed et al. also studied the long-term stability of the electrocatalyst which is considered as an important parameter and was examined by applying cyclic voltammetry and chronoamperometry techniques.

The literature survey shows that many investigators have mostly used carbon blacks as supports. These supports include: Acetylene Black (BET Area:  $50m^2/g$ ), Vulcan XC-72 (BET Area:  $250m^2/g$ ), Ketjen Black (BET Area:  $\approx 900m^2/g$ ) [44] and most recently carbon nanotubes were employed as a good catalyst support [36, 38, 39, 41]. Literature survey also shows that comparative study on synergic metal effect on MOR activity in both acidic and alkaline media has not been extensively studied for non-precious metal based nano-catalysts. Therefore, to develop a stable and highly active non-precious metals nano-catalyst for MOR, it is very important to consider the syn-

thesis method in order to obtain a highly dispersed catalyst with high graphitic content [45].

## **2.2 Carbon Nanotubes**

Carbon nanotubes (CNTs) are a new class of lightweight materials that possess extraordinary mechanical, electrical and thermal properties [46]. They are formed from sheets of graphite that are rolled into a tube and are considered as nearly one-dimensional structures according to their high length to diameter ratio. The most important are single walled nanotubes (SWCNTs) and multi walled nanotubes (MWCNTs) which have cylindrical graphite sheets with nano-meter diameter behaving like metallic or semi-conducting wires [47, 48]. These CNTs are been pursued continuously as an alternative catalyst support in fuel cells because of their promotional effect on catalytic activity and enhancement of mass transfer. Also, CNTs demonstrated better resistance to electrochemical corrosion than carbon black (CB) [49, 50]. The utilization of MWCNTs and their composite as catalyst support material for PEMFCs especially the DMFCs has sparked interest due to their unique properties such as high chemical and oxidative ability, strong mechanical strength, good electronic conductivity and high surface area [20, 21]. Fig. 2.6 shows the structure of the two types of carbon nanotubes;

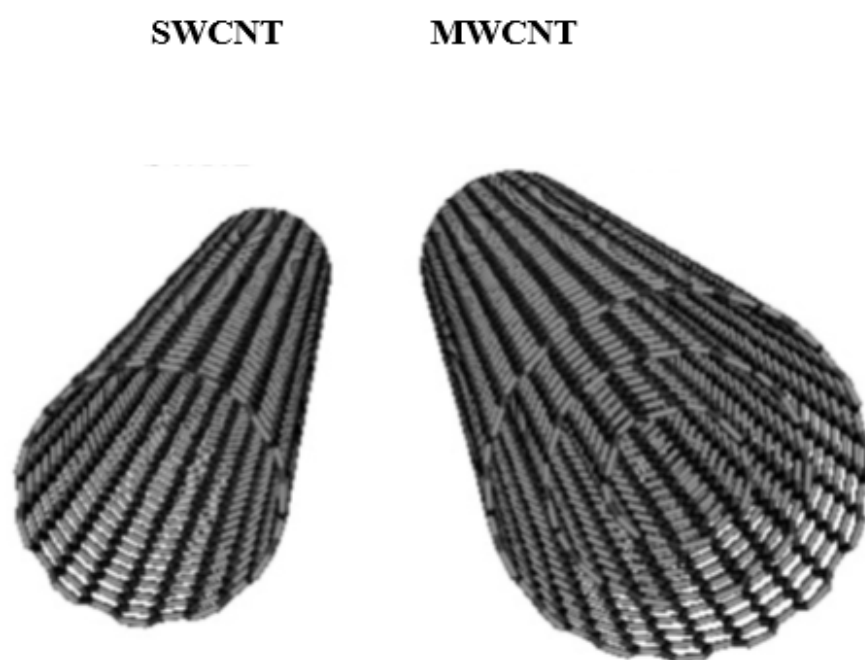


Figure 2.6: Different Types of CNTs

This work focus on development of non-precious metals nano-catalysts using a novel synthesis method to get high yield of highly dispersed nanoparticle catalysts on multi-walled carbon nanotubes support by employing sequential wet impregnation method combined with a freeze-drying procedure.



## CHAPTER 3

# EXPERIMENTAL

### 3.1 Materials

All the chemicals used in this work were of analytical grade. Potassium hydroxide, (85%) was obtained from Winlab Middlesex UK. Copper (II) acetate monohydrate, Nickel (II) nitrate hexahydrate, Nitric acid (65%), Ethanol and Methanol were all obtained from Merck TGaA Germany. Tungsten hexachloride was purchased from BDH Chemicals, Poole England. Sulfuric acid (98%), Hydrochloric acid (37%), Molybdenum (V) chloride and Nafion<sup>®</sup> perfluorinated ion-exchange resin (5wt %) were purchased from Sigma Aldrich St. Louis USA. Multi-walled carbon nanotubes (MWCNTs) purchased from Cheap Tubes Incorporation USA. Milli-Q Q-pod water (Millipore) was used in this work.

## 3.2 Electrocatalysts Synthesis

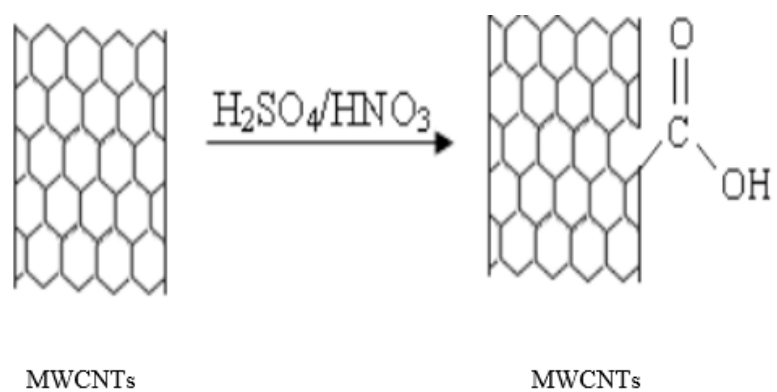
The synthesis of highly dispersed electrocatalyst phase in conjunction with a non-precious metal loading on multi-walled carbon nanotubes (MWCNTs) support is one of the goals of the recent activity in the field of fuel cells technology most especially in DMFCs. In this work, the non-precious metals (NPM) alloy catalysts were prepared, from Ni, Cu, W and Mo as active metals and multi-walled carbon nanotubes as a support. Non-precious bimetallic as well as tri-metallic alloys supported on MWCNTs were prepared and used as electrocatalysts.

## 3.3 CNTs Purification and Functionalization

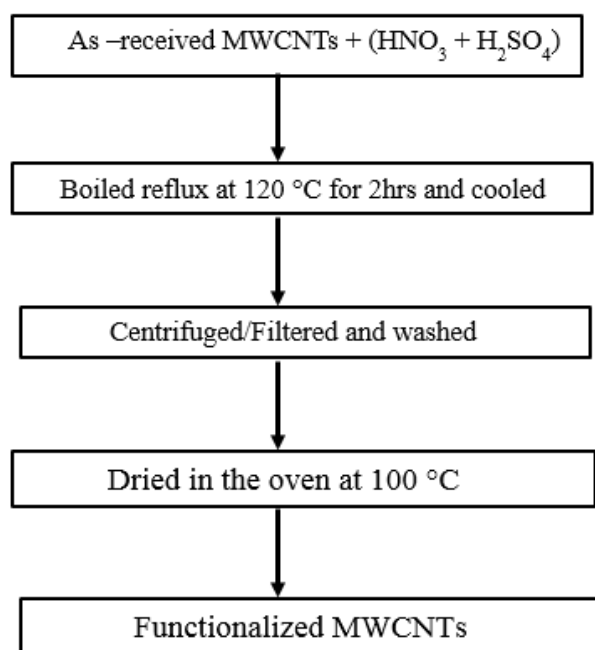
The MWCNTs used in this work were supplied by Cheap Tubes Inc. USA. MWCNTs were produced by chemical process termed combustion chemical vapor deposition (CCVD). Yu et al. [51] reported the functionalization of CNTs by oxidation in  $HNO_3$  and  $H_2SO_4 - HNO_3$  and this shows a higher capability in yielding a significantly high density of surface functional groups such as carbonyl, carboxyl and hydroxyl. These groups can act as specific active/nucleation sites for a well-dispersed deposition of metal clusters on the surface of CNTs. To achieve the unique electronic and mechanical properties of CNTs, they should be further purified chemically in order to functionalize them properly. CNTs have too little anchor sites in the form of defects and functional groups which initiate a proper attachment with the metallic particles [50, 51]. Therefore, a surface activation step (oxidative method) is essential in order to create surface active/nucleation sites that increase the dispersion of the catalyst metals

on the CNTs surface. The aromatic conjugate ring structure of the CNT surface can be modified by an oxidation process using extremely aggressive reagents ( $HNO_3$  or  $H_2SO_4$  or a mixture of the two), resulting in the formation of some functional groups on its surface such as hydroxyl ( $-OH$ ), carboxyl ( $-COOH$ ) and carbonyl ( $-C=O$ ) in the ratio 4:2:1[52]. These surface functional groups are expected to facilitate the chemical interaction between the catalyst metal ions and the modified/functionalized CNTs surface.

The as-received MWCNTs were functionalized using the acid treatment as shown in the Schemes 3.1 and 3.2 below. In a typical procedure, 1g of multi-walled carbon nanotube was treated with mixed acid of 60 ml concentrated sulfuric acid (98%) and 180 ml strong nitric acid (65%). The mixture/suspension was refluxed for 2 hours. Thereafter, the mixture was filtered, washed copiously with de-ionized water and dried in an oven at  $100^\circ C$ . The product obtained was functionalized multi-walled carbon nanotubes.



Scheme 3.1: Functionalization of CNTs



Scheme 3.2: Schematic procedure for functionalization of CNTs

### **3.4 Synthesis Procedure**

The same purification and functionalization process of MWCNTs as well as the synthesis procedure which is sequential wet impregnation method combined with a freeze-drying procedure were employed for the preparation of all the catalyst nano composites. Because a range of catalysts were prepared in this work, few of these catalysts were prepared in various formulations at varying temperatures. Afterwards, those showing low overpotentials and good current flux densities during the electrochemical measurements were chosen and applied in this work.

#### **3.4.1 Sequential Wet Impregnation Method**

Catalysts with metal loading up to 30% were synthesized by using sequential wet impregnation method and the freeze-drying procedure. In this method, a metal salt used as precursor was dissolved in deionized water and then the sample was again impregnated with another metal salt. A measured amount of functionalized MWCNTs was ultrasonically dispersed with an amount of de-ionized water to form slurry. The solution of metal salts was added drop wise to the functionalized MWCNTs slurry and left under magnetic stirring overnight. The metal colloids formed was then vacuum-dried at  $-40^{\circ}\text{C}$  overnight via a freeze drying method to reduce particle agglomeration of the highly dispersed nanoparticle catalyst.

### 3.4.2 Heat Treatment

Finally, the nanoparticles catalysts were systematically heat treated under nitrogen atmosphere at varying temperatures by initially ramping the temperature at  $4^{\circ}\text{C}/\text{min}$  until  $150^{\circ}\text{C}$  where it was held for 30 min. It was finally ramped at  $5^{\circ}\text{C}/\text{min}$  until the target temperature was reached and kept at this temperature for 90 min. The MTI furnace used for the heat-treatment of the nanoparticles catalysts is represented in the Figure 3.1 below. Also the schematic synthetic procedure is given in the scheme 3.3 below and Table 3.1 shows the catalysts synthesized in this work.

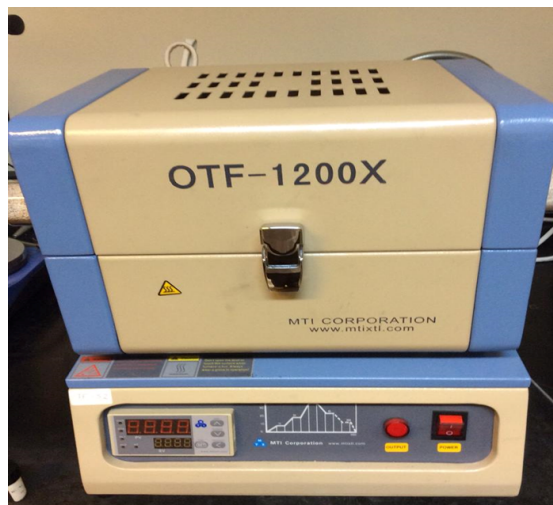
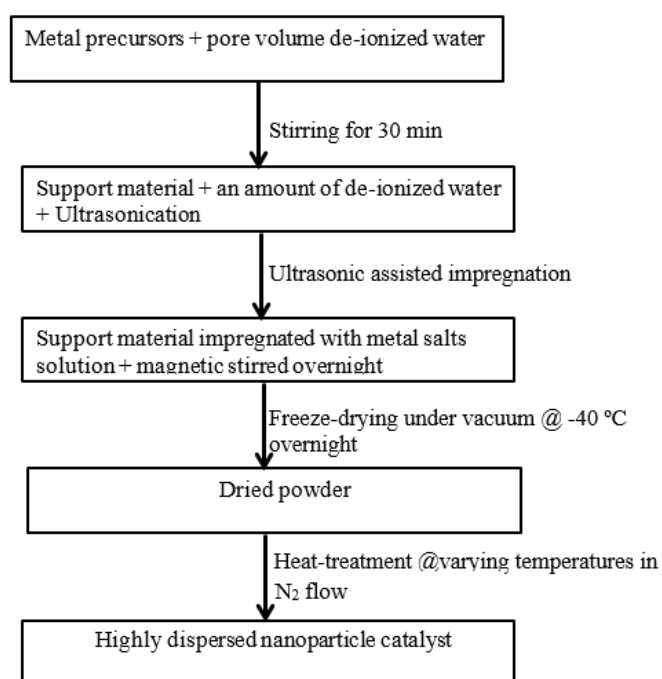


Figure 3.1: High Temperature Vacuum tube furnace used for the heat treatment of the synthesized catalysts





Scheme 3.3: Sequential Wet Method + Freeze Drying Procedure for Metal Supported Catalyst Synthesis

**Table 3.1: Catalysts synthesized in this work at varying composition and heat-treatment**

<b>Catalyst Sample</b>	<b>Heat –Treatment Temperatures</b>
<b>Nickel, Copper loaded on MWCNTs</b>	
70%Ni/30%Cu/MWCNTs	700 °C, 900 °C, 1100 °C
80%Ni/20%Cu/MWCNTs	700 °C, 900 °C, 1100 °C
90%Ni/10%Cu/MWCNTs	700 °C, 900 °C, 1100 °C
<b>Nickel, Copper and Molybdenum loaded on MWCNTs</b>	
70%Ni/20%Cu/10%Mo/MWCNTs	700 °C, 900 °C, 1100 °C
80%Ni/10%Cu/10%Mo/MWCNTs	700 °C, 900 °C, 1100 °C
90%Ni/5%Cu/5%Mo/MWCNTs	700 °C, 900 °C, 1100 °C
<b>Nickel, Copper and Tungsten loaded on MWCNTs</b>	
70%Ni/20%Cu/10%W/MWCNTs	700 °C, 900 °C, 1100 °C
80%Ni/10%Cu/10%W/MWCNTs	700 °C, 900 °C, 1100 °C
90%Ni/5%Cu/5%W/MWCNTs	700 °C, 900 °C, 1100 °C

### 3.5 Electrocatalytic activity measurements

Electrochemical studies were carried out using Bio-Logic Potentiostat SAS, VMP3 France. The electrochemical behaviors of synthesized catalysts, their stabilities and catalytic activities in methanol oxidation (MOR) were investigated using a thin film rotating disk electrode. A convectional glass cell consisting of a three-electrode system at room temperature was used to evaluate the electrochemical reactivity of the electrocatalysts using cyclic voltammetry as well as chronoamperometry techniques as shown in the Figs 3.2 and 3.3.

#### 3.5.1 Electrode and Ink Preparation

The glassy carbon (GC) rotating disk electrode (5 mm diameter) was first polished to a mirror finish with emery paper and alumina slurry and ultrasonically cleaned in dilute sulfuric acid and in de-ionized water for a few minutes and dried in air immediately before being used. For MOR activity measurement, approximately 5 mg of the synthesized catalyst Ni-Mx/MWCNTs/Ni-Mx-My/MWCNTs ( $Mx = Cu$ ,  $My = Mo/W$ ) was dispersed in a mixture of ethanol and de-ionized water (20 % v/v) and 40  $\mu l$  of Nafion<sup>®</sup> (prepared from 5 wt. %, Aldrich).

The mixture was ultra-sonicated for 15 to 30 min to obtain a uniform ink. Then, 10  $\mu l$  of the ink suspension was deposited as a thin film onto a pre-cleaned glassy carbon rotating disk electrode surface (5 mm outer diameter and geometrical  $area = 0.196 cm^2$ , Pine Instruments) and allowed to dry under air flow to prepare the catalyst film impregnated on the glassy carbon rotating disk electrode.

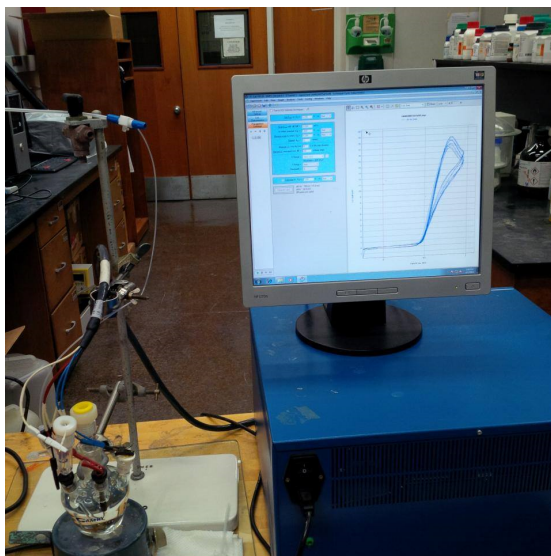


Figure 3.2: A laboratory set-up for electrochemical measurement

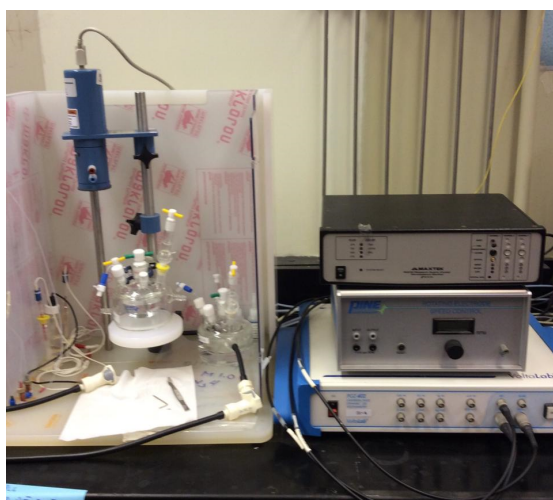


Figure 3.3: A laboratory set-up for electrochemical measurement (catalyst stability)

The loading operation was repeated until the desired catalyst loading,  $0.202\text{mg}/\text{cm}^2$  used for comparison, during this work was achieved.

As a result of the electrochemical measurement trials performed on all the synthesized catalysts, the following synthesized non-precious metals (NPM) catalysts have shown to be promising alternatives to the precious metals catalysts especially Pt based ones.

These (NPM) catalysts are shown in the Table 3.2.

**Table 3.2: Catalysts synthesized for further work at varying composition and heat-treatment**

<b>Catalyst Sample</b>	<b>Heat –Treatment Temperatures</b>
<b>Nickel, Copper loaded on MWCNTs</b>	
90%Ni/10%Cu/MWCNTs	900 °C
90%Ni/10%Cu/MWCNTs	1100 °C
<b>Nickel, Copper and Molybdenum loaded on MWCNTs</b>	
80%Ni/10%Cu/10%Mo/MWCNTs	900 °C
80%Ni/10%Cu/10%Mo/MWCNTs	1100 °C
<b>Nickel, Copper and Tungsten loaded on MWCNTs</b>	
90%Ni/5%Cu/5% W/MWCNTs	900 °C
90%Ni/5%Cu/5% W/MWCNTs	1100 °C

## **CHAPTER 4**

# **RESULTS AND DISCUSSION**

### **4.1 Characterization of the highly dispersed Ni-based catalysts**

The potentiality of the active sites of the highly dispersed Ni-based catalysts in the oxidation of methanol was investigated. Spectroscopic studies were carried out to determine the morphology and the microstructure of these catalysts. Moreover, their elemental composition was also investigated.

### **4.2 Physical Characterization of the Ni-Cu/MWCNTs Catalyst**

The results obtained from various spectroscopic studies as well as electrochemical measurements of Ni-Cu/MWCNTs are discussed as follows;

### 4.2.1 X-Ray Diffraction (XRD) Analysis

For the XRD analyses, used is made of a Rigaku Mini Flex II X-ray diffractometer with a monochromator of  $Cu\ K\alpha1$  ( $\lambda = 1.5406\text{\AA}$ ) generated at 30 kV and 15 mA. The X-Ray patterns were recorded in static scanning mode of  $10^{\circ}\text{C}$  to  $90^{\circ}\text{C}$  ( $2\theta$ ) at a detector angular speed of  $5^{\circ}\text{min}^{-1}$  and step size of  $0.03^{\circ}$ . The XRD is employed to obtain the arrangement of particles in a solid sample. The wavelength of the X-ray is approximately the same as the distance between the particles in the crystal lattice. If the beam of X-ray strikes a crystal, the X-rays are deflected by the crystal and are detected by a photographic plate. This XRD technique was used to investigate the morphology as well as the degree of alloying in the catalyst synthesized. Fig 4.1 shows the X-ray diffraction (XRD) patterns of the synthesized catalyst (Ni-Cu/MWCNTs) composite at varying temperatures. The broad peaks at  $2\theta = 25.787^{\circ}$  are associated with the (002) planes of the graphite-like structure of the multi-walled carbon nanotubes [53, 54]. The analysis demonstrates that the characteristic peaks of the face centered cubic (fcc) crystalline Ni corresponds to the planes (111), (200) and (220) at  $2\theta$  values of about  $44.315^{\circ}$ ,  $51.611^{\circ}$  and  $76.067^{\circ}$  respectively as reported in literature [37]. The slight shifts of the diffraction peaks indicate that the Cu particle has entered into the Ni lattice and thus, there is a formation of an alloy between Ni and Cu [55]. This is a clear evidence that the Ni-Cu alloy particles have been successfully deposited on the MWCNTs.



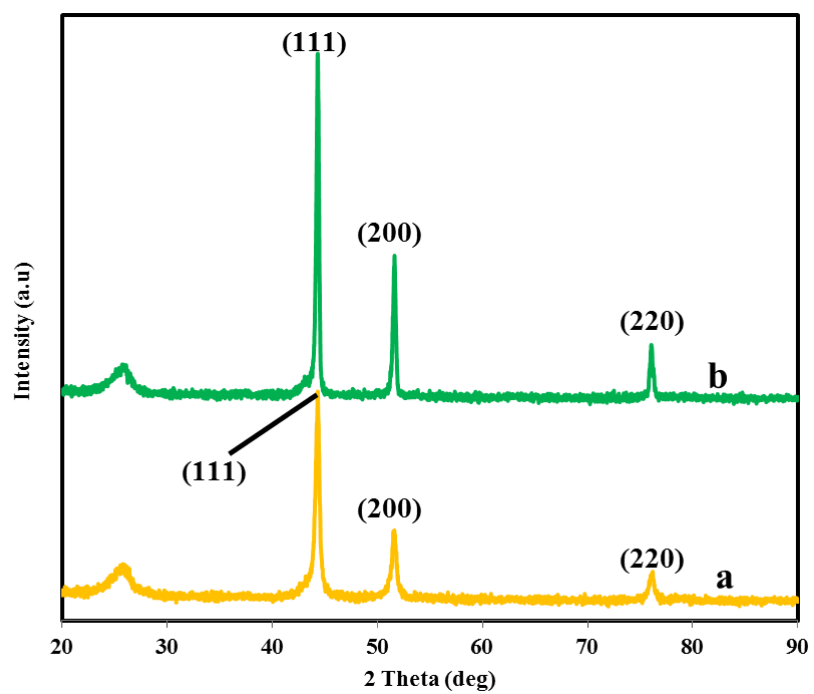


Figure 4.1: X-ray diffraction (XRD) patterns of Ni-Cu/MWCNTs alloy catalyst at 900 °C (a) and 1100 °C (b)

### 4.2.2 FE-SEM Analysis

High-end-field emission scanning electron microscope (FE-SEM JEOL JSM-6610LV, Japan) was used to obtain the FE-SEM micrographs of the synthesized alloy catalysts. The FE-SEM machine uses a focus beam of high-energy electrons to generate a variety of signals at the surface of solid specimens. The signals that are obtained from the electron sample interactions reveal information about the specimen which includes the external/surface morphology (texture), the chemical composition, the crystalline structure and the orientation of materials comprising the catalyst sample. The accelerated electrons in a FE-SEM machine carry large amounts of kinetic energy, which decreases gradually due to the interaction of the incident electrons with the solid samples. The various signals which include secondary electrons (produce the FE-SEM micrographs) were produced. The secondary electrons are most important for showing surface morphology and topography on the solid samples. Figure 4.2 shows the FE-SEM micrographs of the synthesized catalyst (Ni-Cu/MWCNTs) with the high magnification of 20m scale bar. The FE-SEM micrographs clearly reveal the porous structure of the synthesized alloy catalyst. The porous alloy catalysts have been reported elsewhere and have demonstrated high methanol oxidation reaction (MOR) activity than the dense catalysts.

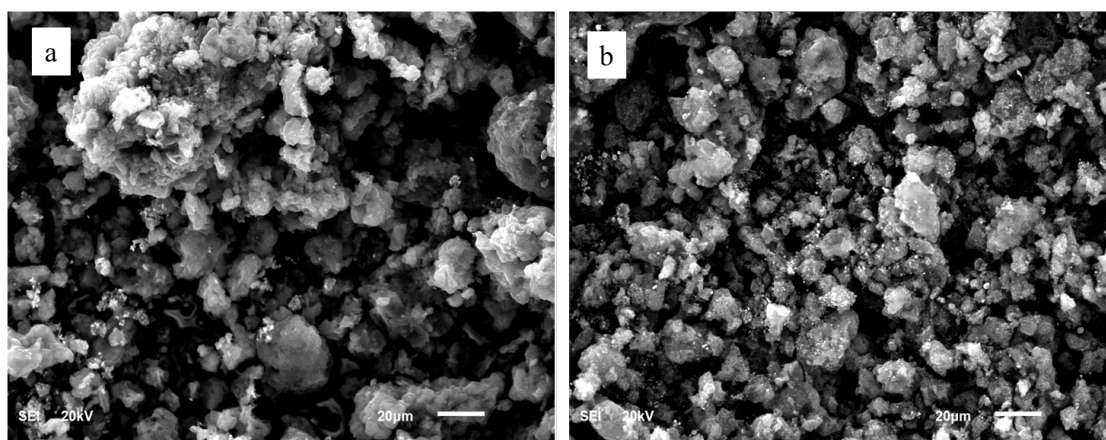


Figure 4.2: FE-SEM micrographs of Ni-Cu/MWCNTs alloy catalyst at 900°C (a) and 1100°C (b)

### 4.2.3 Elemental Analysis

**EDX Analysis:** The Energy dispersive X-ray spectroscopy (EDX, Oxford-Xmax) attached to FE-SEM JEOL JSM 6610LV was used to give information about the preliminary elemental composition of the synthesized catalysts. The identified elements of all the synthesized catalysts were in good agreement with other spectroscopic data (XRD) obtained. The EDX spectrum (Fig 4.3 shows peaks of C, Ni and Cu which was the synthesized catalyst composition and Table 4.1 and 4.2 below shows the percentage composition by weight of the identified elements in the synthesized Ni-Cu/MWCNTs composites. Based on the percentage composition given in the tables, the summary of the average value of each element in each catalyst composite is given in Table 4.3.

**Mapping of Ni-Cu/MWCNTs alloy catalyst:** Energy dispersive X-ray spectroscopy (EDX, Oxford-Xmax) attached to FE-SEM JEOL JSM 6610LV was employed to show the preliminary uniform distribution of the elemental particles present in the synthesized alloy catalysts. Fig 4.4 shows the uniform distribution of Ni and Cu particles on the MWCNTs support surface as evidenced by the elemental mapping using energy-dispersive X-ray spectroscopy.

**ICP-MS Analysis:** The inductively coupled plasma-mass spectroscopy (Thermo Scientific XSERIES 2, USA) was used to estimate the actual metal loaded and the chemical composition of the multi-walled carbon nanotubes supported alloy catalysts. 10 mg of the synthesized alloy catalyst was put into a 50 ml beaker and mixed with a solution containing 12 ml aqua regia (9 ml 37% *HCl* + 3 ml 65%

$HNO_3$ ). Then, the mixture was digested for 75 mins. Afterwards, the solution was filtered into a 25 ml volumetric flask and made up to mark with de-ionized Milli-Pore water as reported elsewhere [56]. The results of ICP-MS analysis obtained were in conformity with the one obtained from the theoretical calculation of atomic ratio for the component elements (i.e Ni and Cu) of the alloy catalyst. The phenomenon further supported the formation of the highly dispersed Ni-Cu/MWCNTs alloy catalyst.

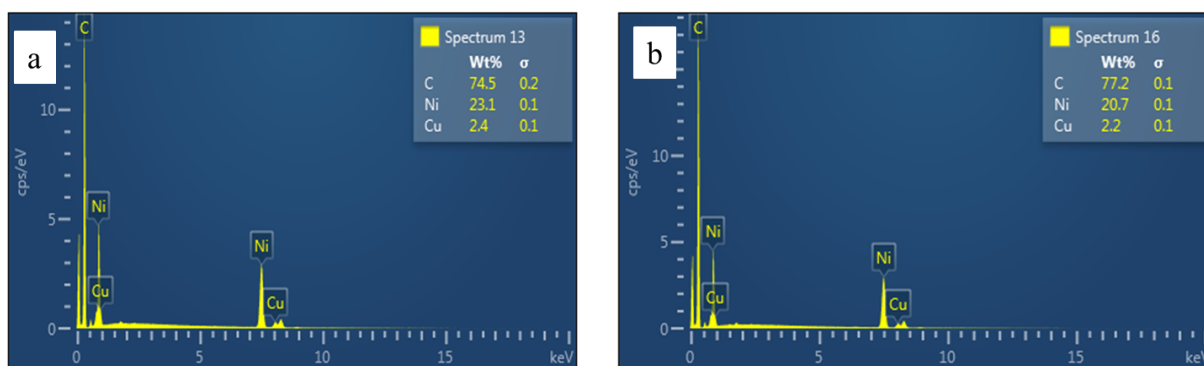


Figure 4.3: EDX Spectrum of Ni-Cu/MWCNTs alloy catalyst at 900°C (a) and 1100°C (b)

Table 4.1: EDX Table showing percentage composition of Ni-Cu/MWCNTs alloy catalyst at 900 °C

Elem	Line Type	App Conc	K Ratio	Wt %	Wt % Sigma	Std Label	Factory Std
C	K Series	65	0.65003	74.48	0.16	C Vit	Yes
Ni	K Series	48.95	0.48950	23.14	0.14	Ni	Yes
Cu	K Series	4.77	0.04767	2.38	0.08	Cu	Yes
Total				100			

Table 4.2: EDX Table showing percentage composition of Ni-Cu/MWCNTs alloy catalyst at 1100 °C

Elem	Line Type	App Conc	K Ratio	Wt %	Wt % Sigma	Std Label	Factory Std
C	K Series	78.05	0.78046	77.18	0.14	C Vit	Yes
Ni	K Series	46.84	0.46839	20.66	0.13	Ni	Yes
Cu	K Series	4.64	0.04644	2.16	0.07	Cu	Yes
Total				100			

Table 4.3: Summary of the average percent by weight of the elements in each alloy catalyst composite

Catalyst	C	Ni	Cu
90%Ni10%CuMWCNTs(900 °C)	65	48.95	4.77
90%Ni10%CuMWCNTs(1100 °C)	78.05	46.84	4.64

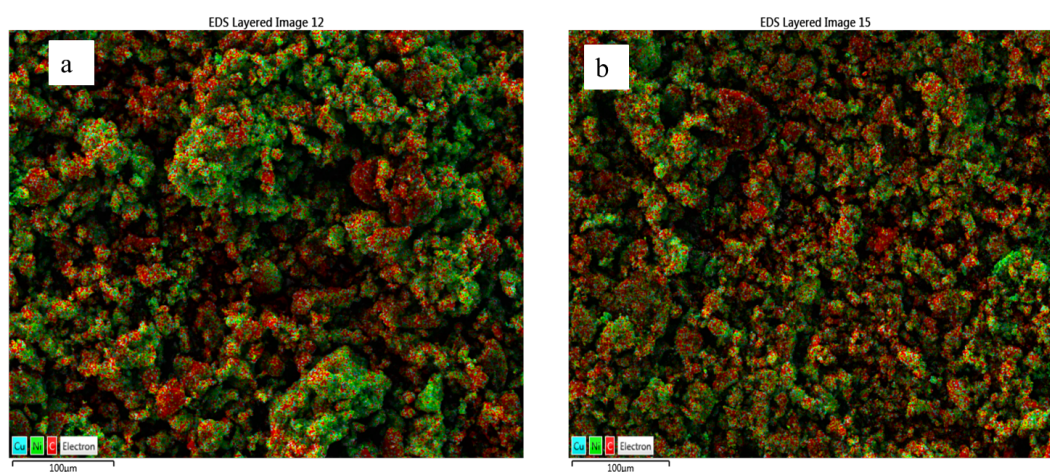


Figure 4.4: Elemental Mapping of Ni-Cu/MWCNTs alloy catalyst at 900°C (a) and 1100°C (b)



#### 4.2.4 FE-TEM Analysis

Field emission-transmission electron microscope (JEOL JEM 2100F, Japan) was used to obtain high resolution transmission electron microscopy (HRTEM) micrographs of the alloy catalyst composites with an excitation voltage of 200 keV. The TEM micrographs of the best synthesized alloy catalyst composites were taken to have indepth understanding of the composition, morphology and the particle size distribution of the catalyst structure. TEM specimens for analysis were prepared by making suspension of synthesized catalysts powder in ethanol and a drop of the suspension was deposited on a standard carbon-covered copper grid (200-mesh). The suspension was allowed to dry so as to evaporate the ethanol and leave the catalyst particles dispersed on the grid before insertion into the microscope. The HRTEM micrographs (Fig 4.5) below show that Ni-Cu nanoparticles are decorated on the MWCNTs support which indicate that there is a homogenous dispersion of the nanoparticles, largely spherical particles. The nanoparticles aggregates have not been observed. This is probably due to the effect of surface functional groups (specific nucleation sites), such as ( $-COOH$ ), ( $-C=O$ ) and ( $-OH$ ) groups which may help the metal nanoparticles to be adsorbed onto the MWCNTs surface via hydrogen bonding [57, 58].

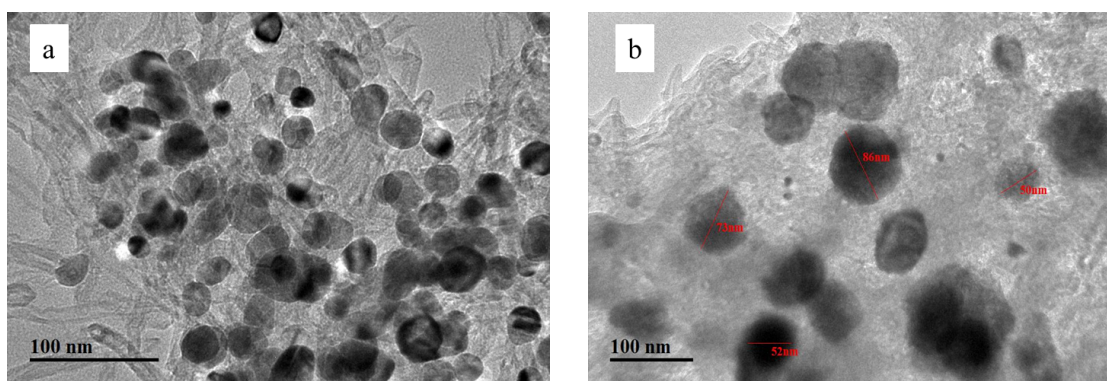


Figure 4.5: HR-TEM micrographs of Ni-Cu/MWCNTs alloy catalyst at 900°C (a) and 1100°C (b)

#### 4.2.5 BET Analysis of MWCNTs

The Brunauer–Emmett–Teller (BET) measurements of MWCNTs were investigated by using ASAP-220 surface Area and Porosity Analyzer from micrometrics. The BET surface area of the carbon support that is the as-received MWCNTs and the functionalized MWCNTs, as well as their pore volume and pore size was measured (Table 4.4). The BET surface area of the functionalized MWCNTs is much lower compare to the as-received MWCNTs; this is as a result of the surface coverage by the surface functional groups (-COOH, -OH and =CO) which make the functionalized MWCNTs to be mesoporous. The pore volume and pore size of the functionalized MWCNTs are lower to that of the as-received MWCNTs due to pore coverage and according to IUPAC standard porosity ranges between 2 nm and 50 nm. Based on this, the material with less than 2 nm is micropore while one above 50 nm is macropore.

Table 4.4: BET Analysis table showing the BET surface area, pore volume and pore size of MWCNTs

	As-Received MWCNTs	Functionalized MWCNTs
BET surface area ( $m^2/g$ )	183.03	155.38
Pore volume ( $cm^3/g$ )	0.726	0.422
Pore size (nm)	15.8	10.8

### 4.3 Cyclic Voltammogram in $N_2$ saturated solution

Before methanol oxidation reaction measurements, the potential of the polished glassy carbon electrode was cycled in nitrogen saturated 0.1 M KOH for 15-20 cycles at 20 mV/s until a stabilized Cyclic Voltammogram (CV) was recorded. Also, the reference electrode was calibrated versus a dynamic hydrogen electrode using a platinum electrode with hydrogen gas bubbling through 0.1 M KOH electrolyte at 25°C. All the measured potentials were recorded versus this electrode (+0.951 V vs RHE). The cyclic voltammetry was conducted in a glass cell consisting of a three-electrode system in 0.5 M  $CH_3OH$  + 0.1 M  $KOH$  solution at 25°C in deaerated conditions under  $N_2$  gas. The working electrode was the catalyst supported glassy carbon rotating disk electrode, the counter electrode was a platinum wire mesh and a Ag/AgCl (in 3 M KCl) electrode was used as a reference electrode. Fig. 4.6 shows cyclic voltammograms of Ni-Cu/MWCNTs electrode formulations of different heat treatments in a -0.2 to 1.0 V potential range (Vs Ag/AgCl) at a 20 mV/s scan rate in 0.5 M  $CH_3OH$  + 0.1 M  $KOH$  solution and Fig 4.7 represents the cyclic voltammetric curves of methanol oxidation (0.5 M) at different temperatures for Ni-Cu/MWCNTs electrode in a -0.2 to 1.0 V potential range (vs Ag/AgCl) at a 20 mV/s scan rate in 0.1 M KOH.

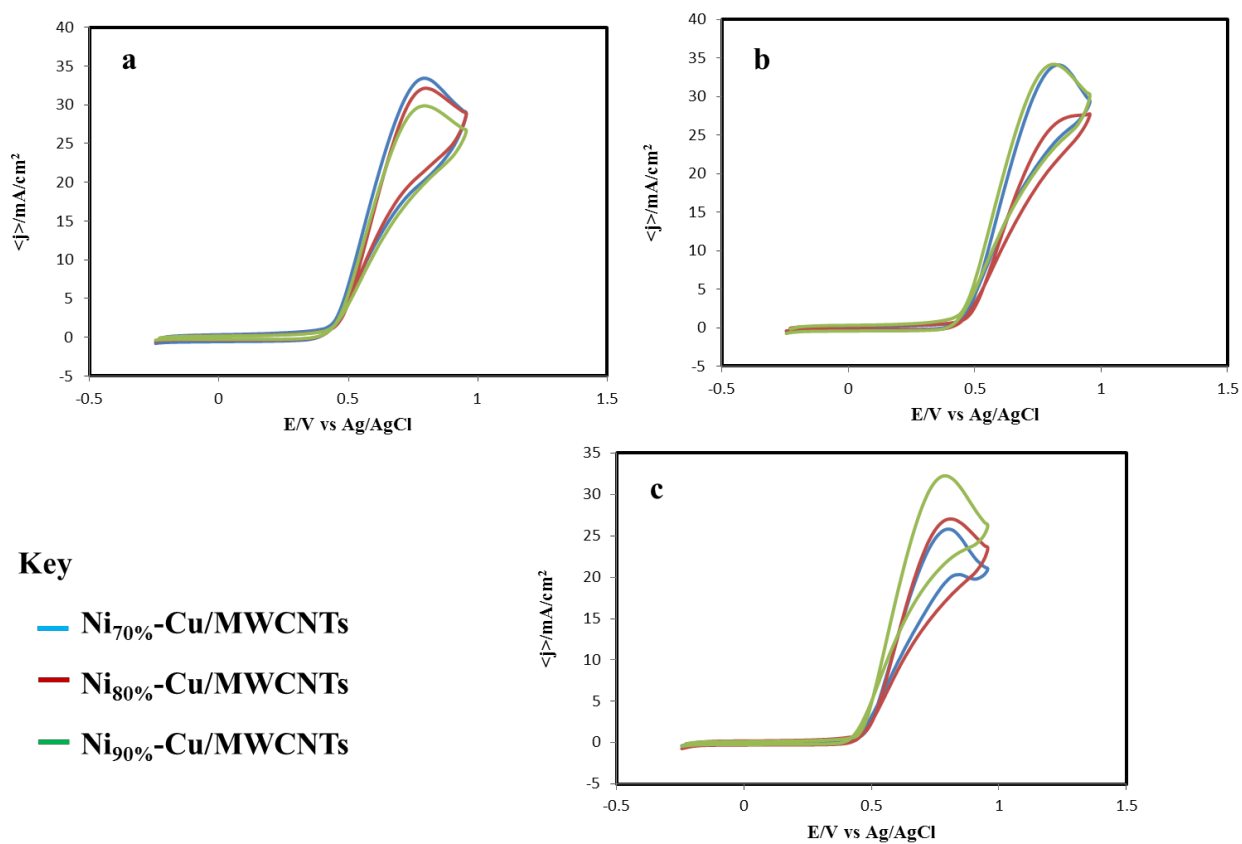


Figure 4.6: Cyclic voltammograms of Ni-Cu/MWCNTs electrode formulations at 700°C (a), 900°C (b) and 1100°C (c) in 0.5 M  $CH_3OH$  + 0.1 M  $KOH$  at a scan rate of 20mV/s

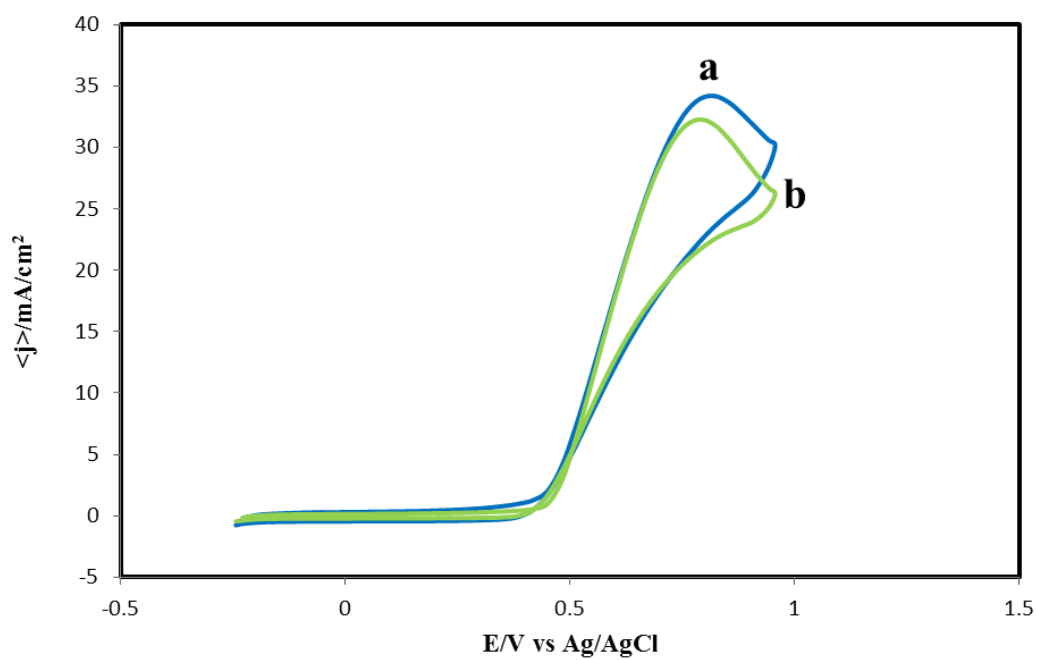


Figure 4.7: Cyclic voltammograms of Ni-Cu/MWCNTs electrode at 900 °C (a) and 1100 °C (b) in 0.5 M  $CH_3OH$  + 0.1 M  $KOH$  at a scan rate of 20 mV/s

### 4.3.1 Effect of Ni-Cu/MWCNTs Alloy Catalyst Loading

The electroactivity of Ni-Cu/MWCNTs alloy catalyst in the oxidation of methanol was evaluated in 0.1 M KOH solution saturated with  $N_2$  using catalyst loadings of  $0.2\text{mg}/\text{cm}^2$  and  $0.4\text{mg}/\text{cm}^2$  respectively. The cyclic voltammetric curves obtained are shown in Figure 4.8. It can be observed that the current flux density decreases with increasing the catalyst loading and the MOR on-set potentials have no significant change with the catalyst loading at  $900^\circ\text{C}$ . Moreover, no much significant change was noticed for the catalyst at a temperature of  $1100^\circ\text{C}$ .

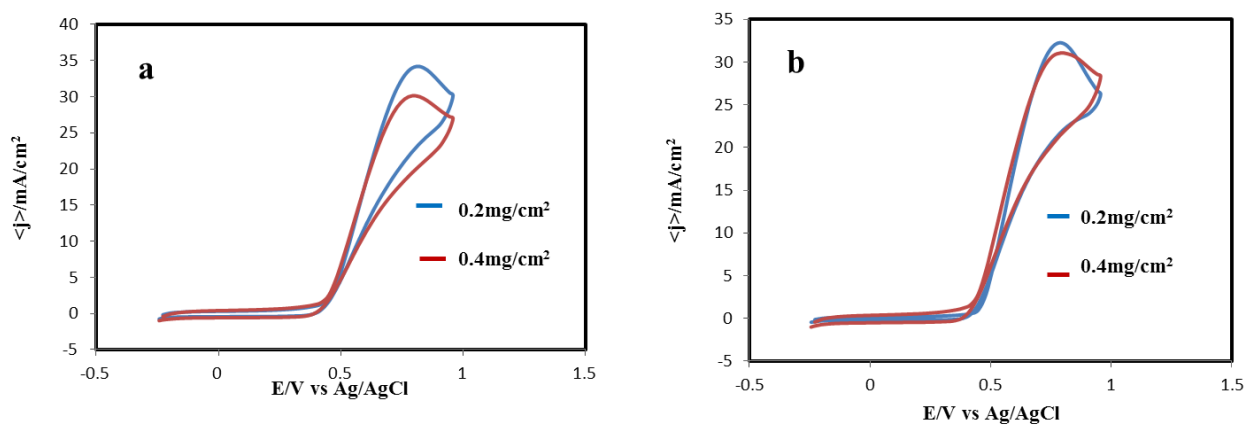


Figure 4.8: Cyclic voltammograms of Ni-Cu/MWCNTs catalyst loading at 900°C (a) and 1100°C (b) in 0.5 M  $\text{CH}_3\text{OH}$  + 0.1 M  $\text{KOH}$  at a scan rate of 20  $\text{mV}/\text{s}$



### **4.3.2 Ni-Cu/MWCNTs Alloy Catalyst Durability**

The catalyst calcinated at high temperature (1100°C) showed not only remarkable activity, but also good stability after being subjected to prolonged potential cycling between 0.20 and 1.0 V/RHE at a scan rate of 20 mV/s in accordance with the DOE protocol. At a constant current flux density (approximately half-wave potential), there is no significant drop in voltage (Figure 4.9). This means that the degradation rate has dropped and such a trend in the activity loss over cycling has also been seen with conventional precious metal catalyst [45], where most of MOR overvoltage occurs in the first 0-1k cycles, after which the activity stabilizes.

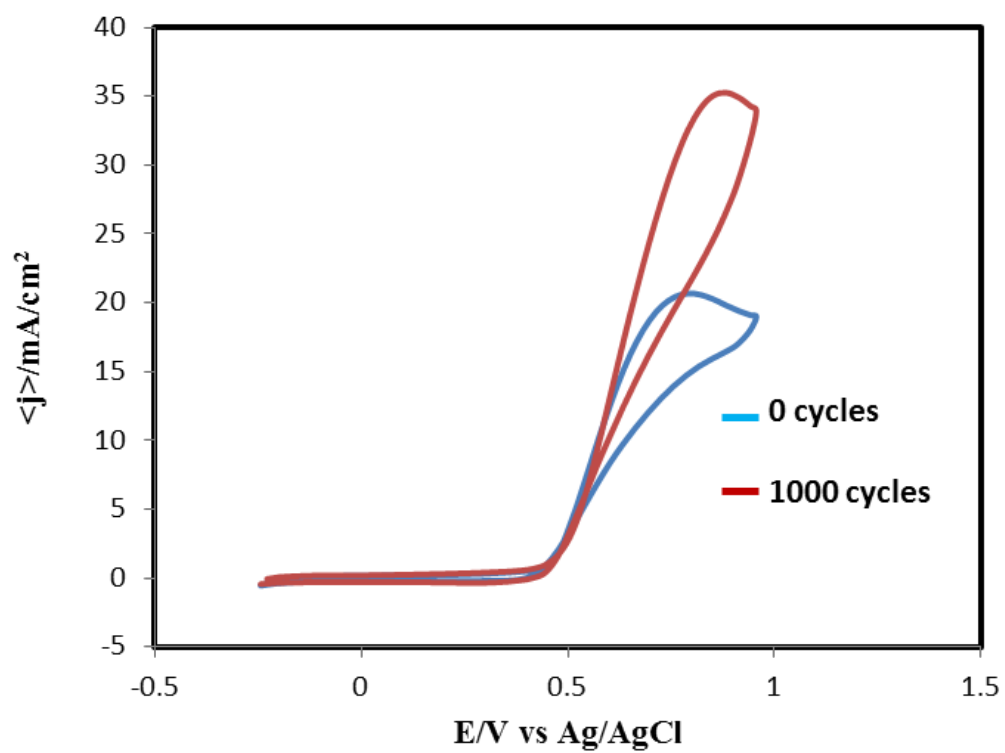


Figure 4.9: Stability Test for Ni-Cu/MWCNTs Cyclic Voltammograms in  $N_2$  saturated 0.5 M  $CH_3OH$  + 0.1 M KOH

Chronoamperometric technique is a good method used to determine the electro-catalytic activity and stability of nano-catalyst materials. Chronoamperometry was performed using Ni-Cu/MWCNTs alloy catalyst of different temperatures for a period of 10 mins at a constant potential (0.65 V vs Ag/AgCl). Fig. 4.10 shows the typical current density-time responses of Ni-Cu/MWCNTs alloy catalysts for methanol electro-oxidation reaction at different temperatures. The two catalysts present gradual current flux decay before a steady current flux status was obtained which was attributed to the formation of some Ni oxides/hydroxides and adsorbed intermediates during the electro-oxidation of methanol [37]. As expected, the methanol electro-oxidation current flux density of the alloy catalyst calcinated at high temperature was evidently higher than that obtained at lower temperature. In the steady-state region, it was observed that Ni-Cu/MWCNTs alloy catalyst calcinated at high temperature presented current flux density of  $30.45\text{mA}/\text{cm}^2$  Ni (decreased 13.93% relative initial current flux density) while the one calcinated at lower temperature exhibited a current flux density of about  $10.85\text{mA}/\text{cm}^2$  Ni (41.51%). The alloy catalyst calcinated at lower temperature shows lowest initial current flux density and limiting current flux density which may be due to the conversion of Ni into nickel oxide/hydroxide which cover the Cu atoms surface in the activation polarization process [59]. Thus, the incomplete oxidation products will be adsorbed on the alloy catalyst surface resulting in the slowing down of the MOR.

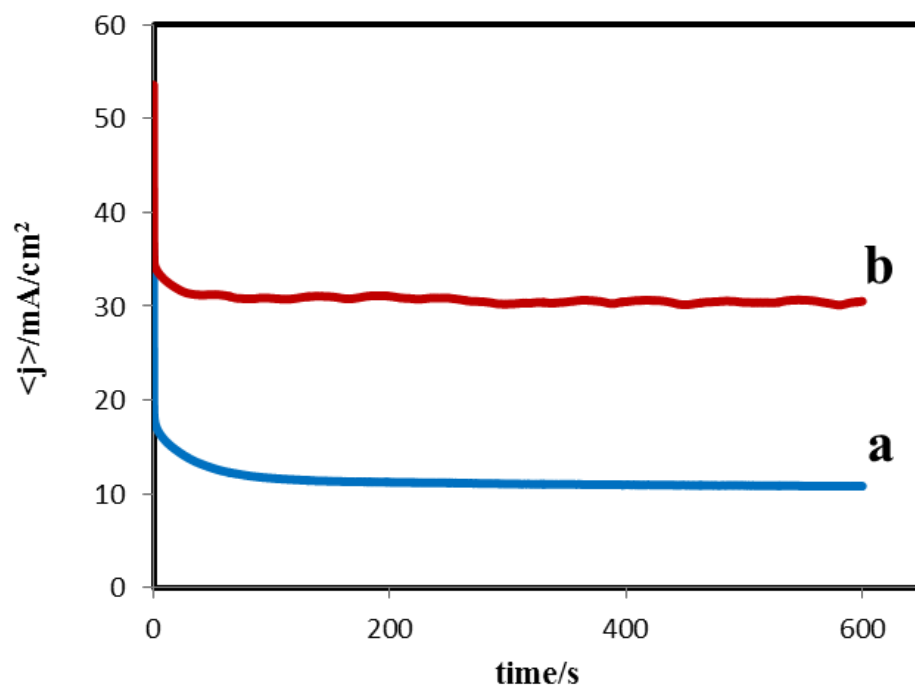


Figure 4.10: Chronoamperometry collected for 10 min at 0.650 V for Ni-Cu/MWCNTs alloy catalyst at 900 °C (a) and 1100 °C (b) in 0.5 M  $\text{CH}_3\text{OH}$  + 0.1 M KOH

## **4.4 Physical Characterization of Ni-Cu-Mo/MWCNTs**

### **Alloy Catalyst**

The results obtained from various spectroscopic studies as well as electrochemical measurements of Ni-Cu-Mo/MWCNTs alloy catalysts are discussed as follows;

#### **4.4.1 X-Ray Diffraction (XRD) Analysis**

Figure 4.11 shows the X-ray diffraction (XRD) patterns of the Ni-Cu-Mo/MWCNTs composite at varying temperatures with broad peaks at  $2\theta = 25.374^\circ$  are associated with the (002) planes of the graphite-like structure of the multi-walled carbon nanotubes. The other three peaks of the Ni-Cu-Mo/MWCNTs composite corresponds to the planes (111), (200) and (220) at  $2\theta$  values of about  $44.048^\circ$ ,  $51.319^\circ$  and  $75.683^\circ$  respectively [37]. The slight shifts of the diffraction peaks reveal that partial Cu and Mo have entered into the Ni lattice and results to the formation of Ni-Cu-Mo alloy on the multi-walled carbon nanotubes surface.

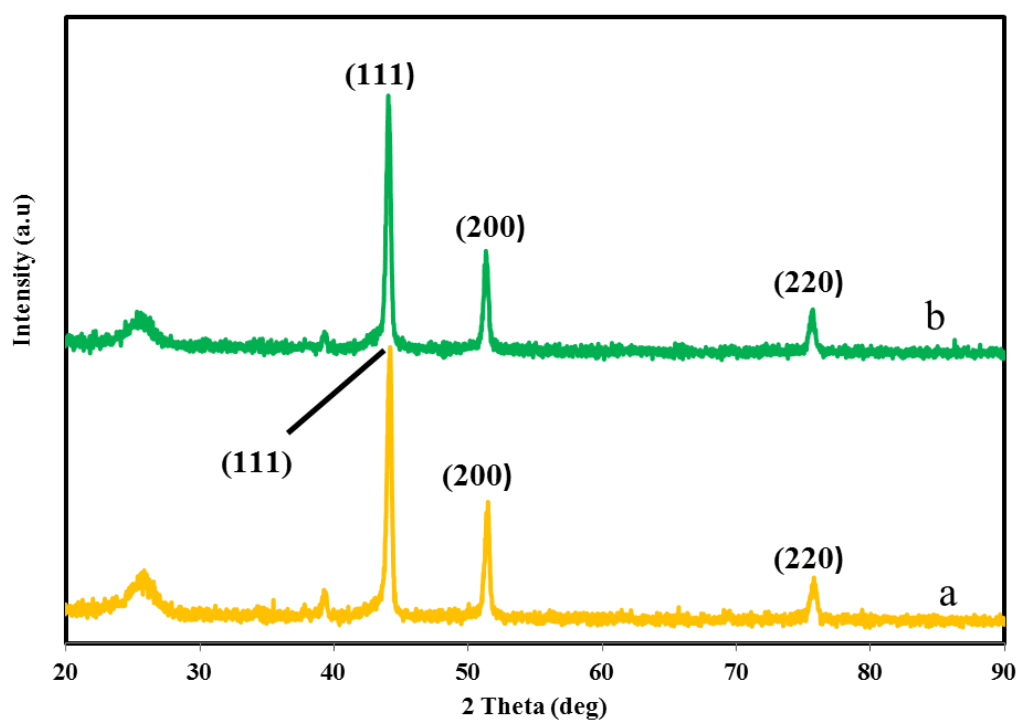


Figure 4.11: X-ray diffraction (XRD) patterns of Ni-Cu-Mo/MWCNTs alloy catalyst at 900°C (a) and 1100°C (b)

#### **4.4.2 FE-SEM Analysis**

The FE-SEM micrographs of the highly dispersed Ni-Cu-Mo/MWCNTs show that more metal nanoparticles exhibit very well uniform dispersion on the surface of the functionalized MWCNTs (Fig 4.12). The SEM images of the synthesized catalysts at higher magnification of  $20\mu m$  scale bar reveal good porous structure which has been well reported elsewhere to have demonstrated high MOR activity than the dense ones.

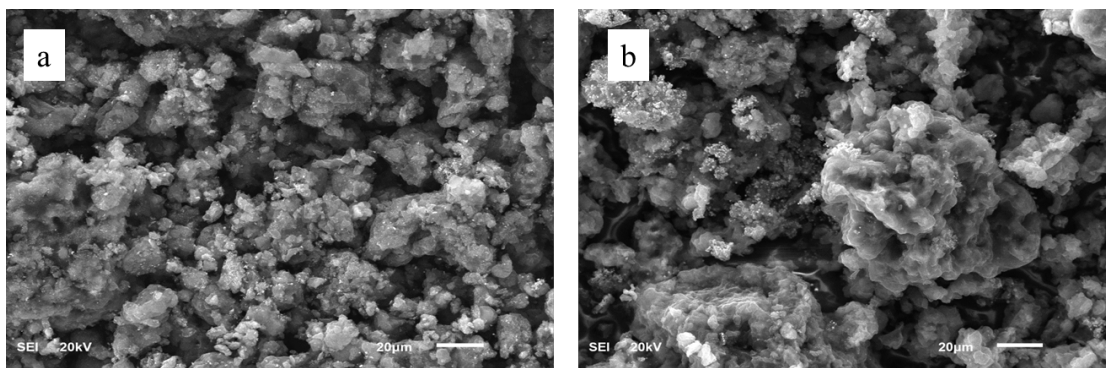


Figure 4.12: SEM micrographs of Ni-Cu-Mo/MWCNTs alloy catalyst at 900°C (a) and 1100°C (b)



#### 4.4.3 Elemental Analysis

**EDX Analysis:** The energy-dispersive X-ray spectroscopy (EDX) analysis (Fig. 4.13) was applied to determine the major elements in the Ni-Cu-Mo/MWCNTs catalyst. Thus, the EDX spectrum shows peaks of C, Ni, Cu and Mo which represent the major constituents of the synthesized catalyst and Table 4.5 and 4.6 shows the percentage composition by weight of the identified elements in the synthesized Ni-Cu-Mo/MWCNTs composites. Based on the percentage composition given in the tables, the summary of the average value of each element in each catalyst composite is given in the Table 4.7.

**Mapping of Ni-Cu-Mo/MWCNTs alloy catalyst:** The uniform distribution of Ni, Cu and Mo particles on the MWCNTs support surface was evaluated by elemental mapping using energy-dispersive X-ray spectroscopy attached to FE-SEM JEOL JSM 6610LV machine (Figure 4.14).

**ICP-MS Analysis:** To further evaluate the Ni, Cu and Mo component, ICP-MS technique was employed for the estimation of the chemical composition of the MWCNTs supported Ni-Cu-Mo catalyst. The alloy catalyst was firstly digested in aqua regia, filtered and then made up to the mark in the standard flask with de-ionized Milli-Pore water as reported in literature [56]. The results obtained from this analysis go in line with the one obtained from theoretical calculation of the atomic ratio for the component elements ( i.e Ni, Cu and Mo) of the alloy catalyst and it further supports the formation of the highly dispersed Ni-Cu-Mo/MWCNTs alloy catalyst.

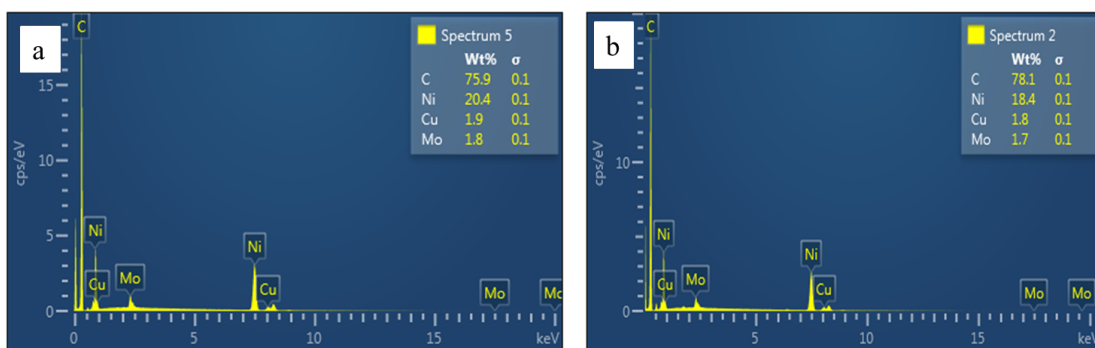


Figure 4.13: EDX Spectrum of Ni-Cu-Mo/MWCNTs alloy catalyst at 900°C (a) and 1100°C (b)

Table 4.5: EDX Table showing percentage composition of Ni-Cu-Mo/MWCNTs alloy catalyst at 900°C

Elem	Line Type	App Conc	K Ratio	Wt %	Wt % Sigma	Std Label	Factory Std
C	K Series	74.5	0.74501	75.86	0.15	C Vit	Yes
Ni	K Series	47.94	0.47937	20.43	0.13	Ni	Yes
Cu	K Series	4.19	0.04190	1.88	0.07	Cu	Yes
Mo	L Series	4.09	0.04089	1.82	0.06	Mo	Yes
Total				100			

Table 4.6: EDX Table showing percentage composition of Ni-Cu-Mo/MWCNTs alloy catalyst at 1100°C

Elem	Line Type	App Conc	K Ratio	Wt %	Wt % Sigma	Std Label	Factory Std
C	K Series	78.51	0.78511	78.1	0.15	C Vit	Yes
Ni	K Series	41.36	0.41361	18.4	0.13	Ni	Yes
Cu	K Series	3.82	0.03815	1.79	0.07	Cu	Yes
Mo	L Series	3.72	0.03725	1.71	0.06	Mo	Yes
Total				100			

Table 4.7: Summary of the average percent by weight of the elements in each alloy catalyst composite

Catalyst	C	Ni	Cu	Mo
90%Ni10%CuMWCNTs(900°C)	74.5	47.54	4.19	4.09
90%Ni10%CuMWCNTs(1100°C)	78.51	41.36	3.82	3.72

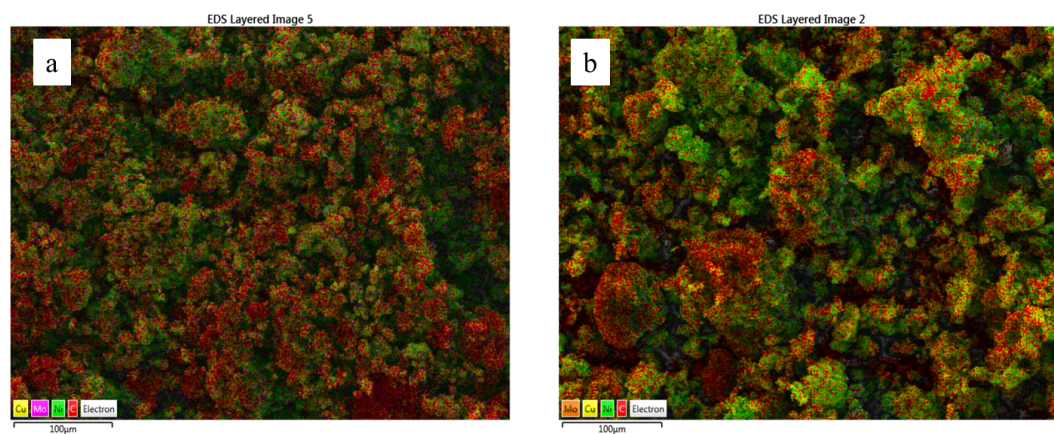


Figure 4.14: Elemental Mapping of Ni-Cu-Mo/MWCNTs alloy catalyst at 900°C (a) and 1100°C (b)

#### **4.4.4 FE-TEM Analysis**

The synthesized catalyst composite morphology and particle size distribution on the multi-walled carbon nanotubes support were investigated using FE-TEM JEOL JEM-2100F, Japan (Fig 4.15). The HRTEM micrographs show that the Ni-Cu-Mo nanoparticles are decorated on the MWCNTs and homogenously dispersed largely in spherical shape. Thus, the aggregation of the metal nanoparticles is rarely observed which can be attributed to the specific nucleation sites such as -COOH, =CO and -OH which may help the metal nanoparticles to be adsorbed onto the MWCNTs surface through hydrogen bonding [57, 58].

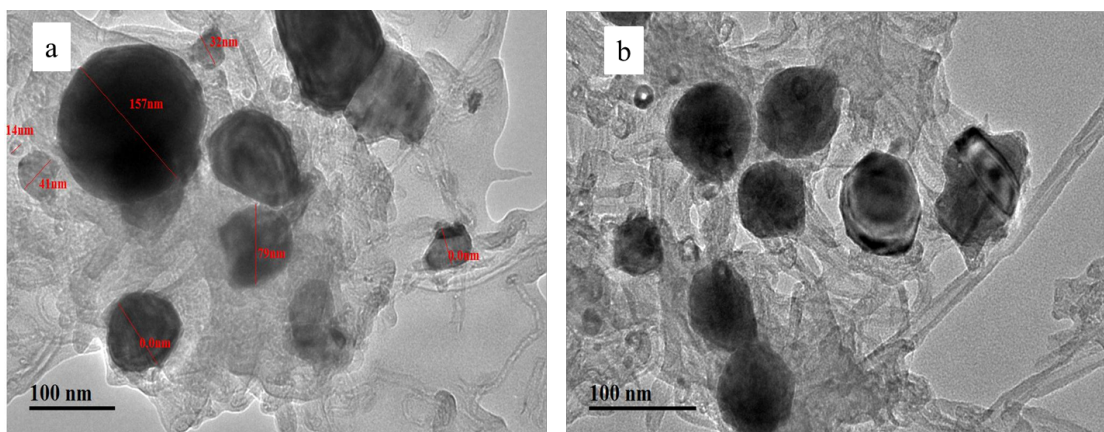


Figure 4.15: HRTEM micrographs of Ni-Cu-Mo/MWCNTs alloy catalyst at 900°C (a) and 1100°C (b)

## 4.5 Cyclic Voltammogram in $N_2$ saturated solution

The same electrochemical measurements were conducted for Ni-Cu-Mo/MWCNTs alloy catalyst of different temperatures. Fig. 4.16 shows the cyclic voltammetric curves of methanol oxidation (0.5 M) for Ni-Cu-Mo/MWCNTs electrode formulations at different heat treatments at a -0.2 to 1.0 V potential range (vs Ag/AgCl) with a 20 mV/s scan rate in 0.1 M KOH and Fig. 4.17 shows the cyclic voltammograms of Ni-Cu-Mo/MWCNTs electrode at different temperatures at a -0.2 to 1.0 V potential range (Vs Ag/AgCl) using a 20 mV/s scan rate in 0.5 M  $CH_3OH$  + 0.1 M  $KOH$  solution.

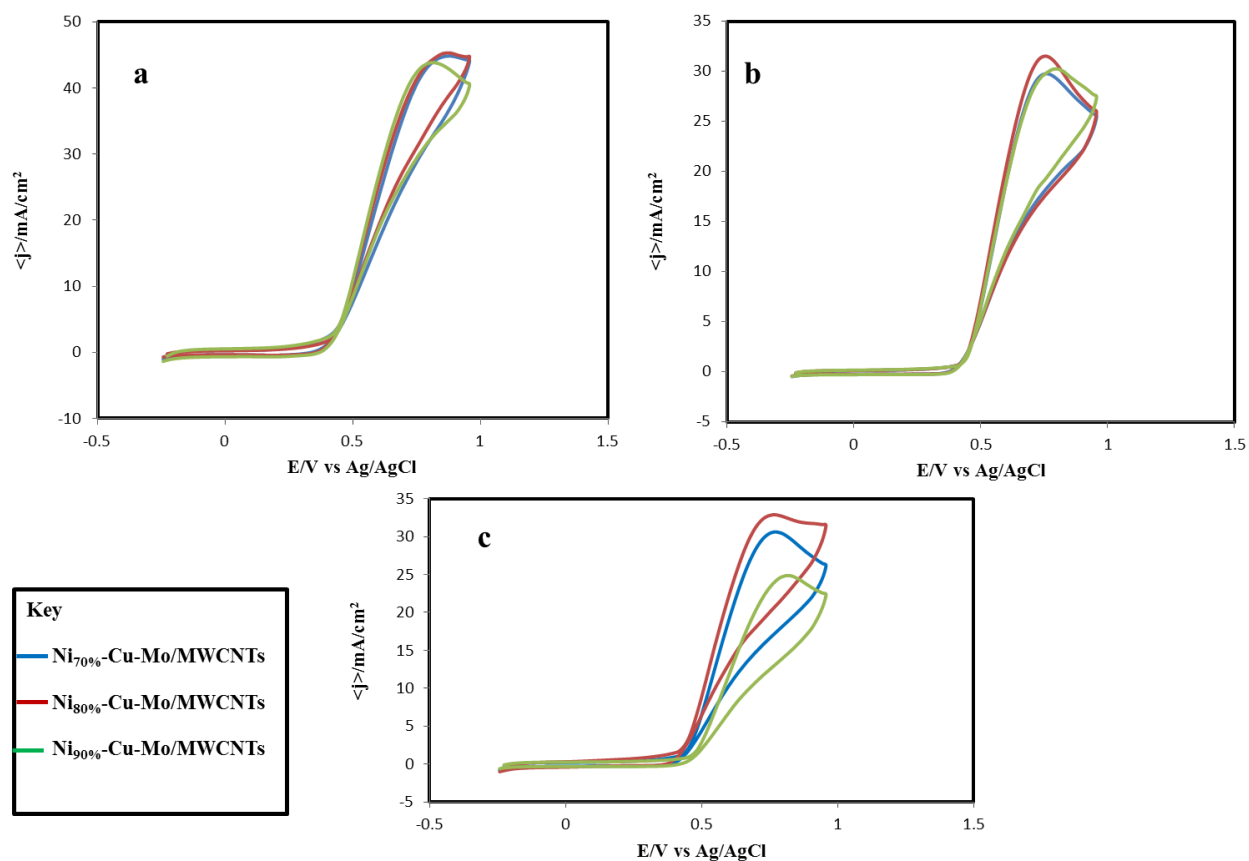


Figure 4.16: Cyclic voltammograms of Ni-Cu-Mo/MWCNTs electrode formulations at 700 °C (a), 900 °C (b) and 1100 °C (c) in 0.5 M  $\text{CH}_3\text{OH}$  + 0.1 M  $\text{KOH}$  at a scan rate of 20 mV/s



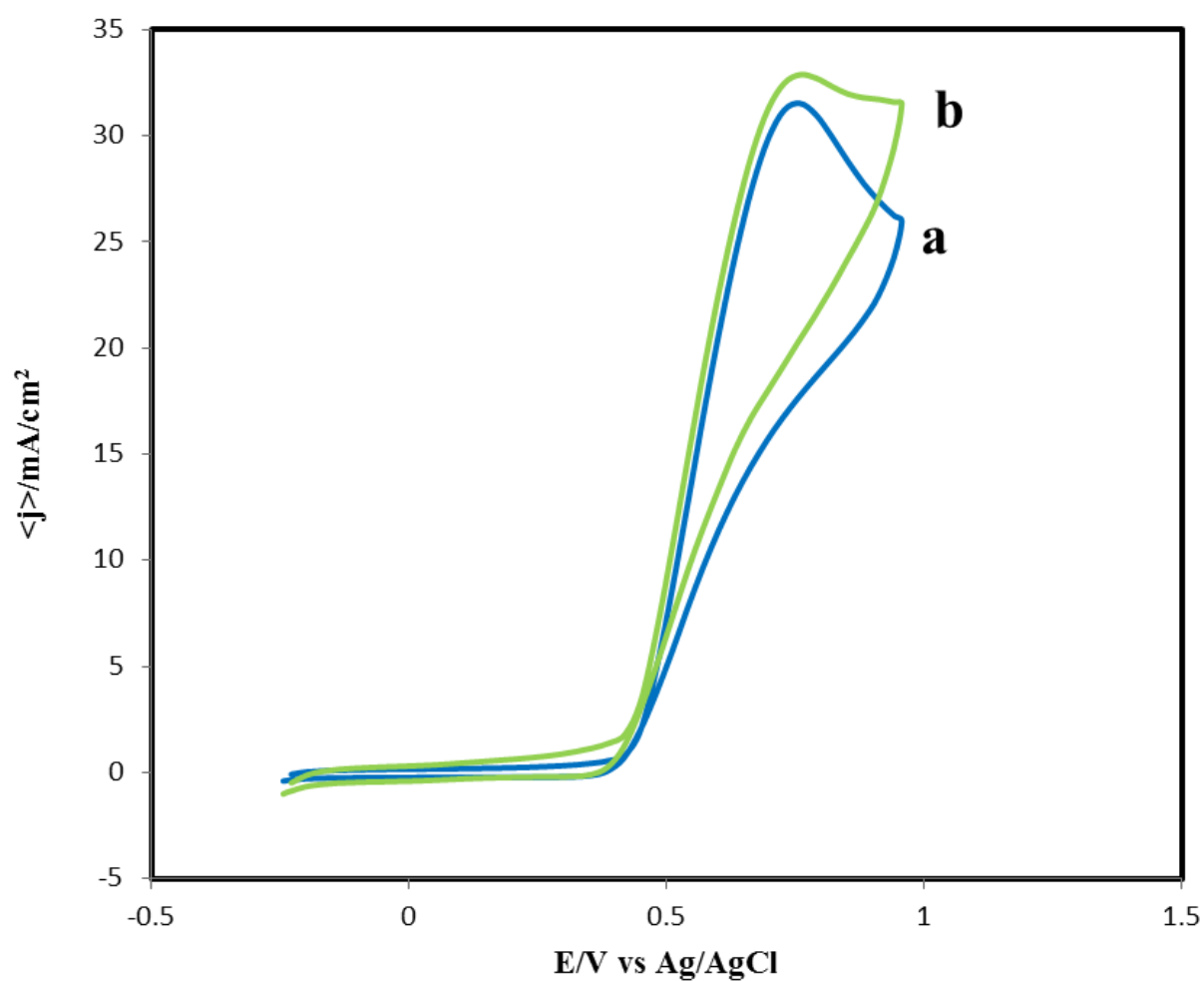


Figure 4.17: Cyclic voltammograms of Ni-Cu-Mo/MWCNTs electrode at 900°C (a) and 1100°C (b) in 0.5 M  $\text{CH}_3\text{OH}$  + 0.1 M  $\text{KOH}$  at a scan rate of 20 mV/s

#### **4.5.1 Effect of Ni-Cu-Mo/MWCNTs Alloy Catalyst Loading**

The methanol oxidation activity of Ni-Cu-Mo/MWCNTs alloy catalyst was evaluated in a nitrogen saturated 0.1 M KOH solution with a catalyst loading of  $0.2\text{mg}/\text{cm}^2$  and  $0.4\text{mg}/\text{cm}^2$  respectively. The cyclic voltammetric curves obtained are shown in Fig. 4.18. It is obvious that the current flux densities have increase with the catalyst loading. However, the MOR on-set potentials have shown no significant change with the catalyst loading. Although, at low catalyst loading the limiting currents were not well- defined but became better as the catalyst loading was increased due to more active sites for the methanol oxidation. High activity obtained during this work especially with Ni-Cu-Mo/MWCNTs, can be attributed to the synergic effect of co-catalyst (Mo) especially at higher catalyst loadings.

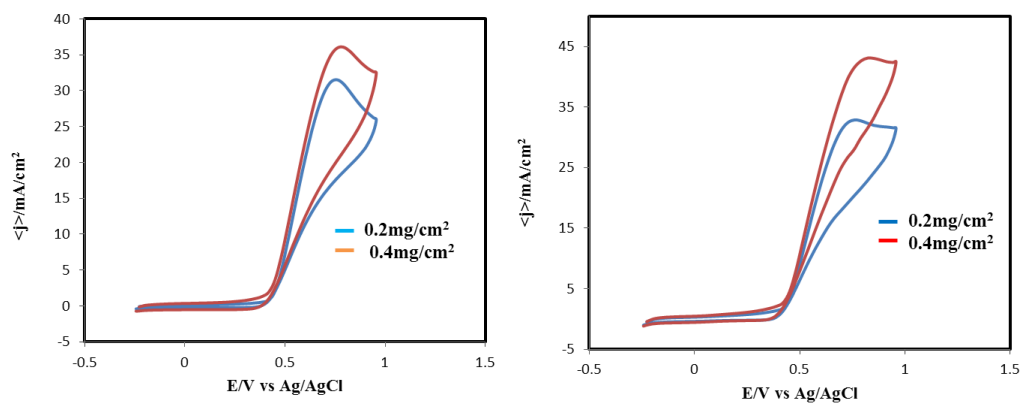


Figure 4.18: Cyclic voltammograms of Ni-Cu-Mo/MWCNTs catalyst loading at  $900^\circ\text{C}$  (a) and  $1100^\circ\text{C}$  (b) in  $0.5\text{ M CH}_3\text{OH} + 0.1\text{ M KOH}$  at a scan rate of  $20\text{mV}/\text{s}$

#### 4.5.2 Ni-Cu-Mo/MWCNTs Alloy Catalyst Durability

The stability of Ni-Cu-Mo/MWCNTs alloy catalyst was investigated by potential cycling in 0.1 M KOH electrolyte in presence of 0.5 M  $CH_3OH$ . The catalyst calcinated at high temperature (1100°C) has shown remarkable activity, in addition to good stability after being subjected to prolonged potential cycling between 0.20 and 1.0 V/RHE at a scan rate of 20mV/s in accordance with the DOE protocol. At a constant current flux density (approximately half-wave potential), there is significant drop in voltage as can be seen from Fig. 4.19.

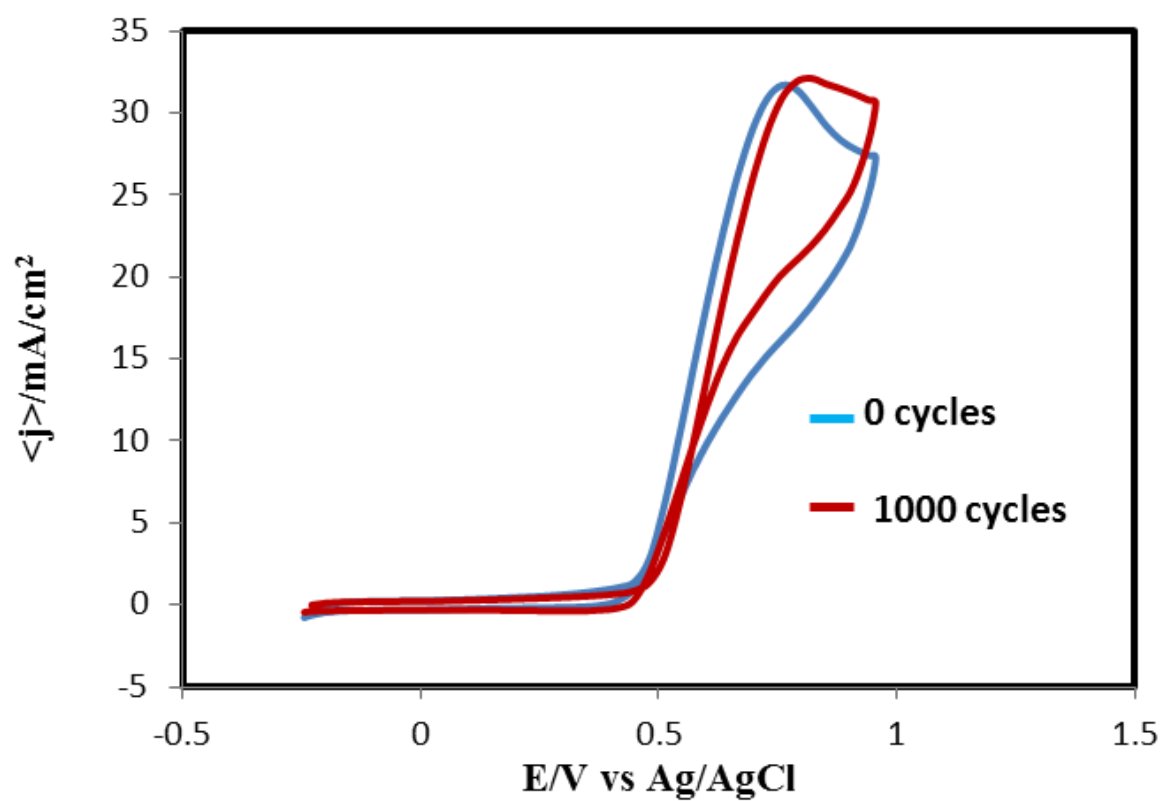


Figure 4.19: Stability Test for Ni-Cu-Mo/MWCNTs Cyclic Voltammograms in  $N_2$  saturated 0.5 M  $CH_3OH$  + 0.1 M  $KOH$

Chronoamperometry was also carried out to evaluate the electrocatalytic activity as well as the stability of the alloy catalyst. It was performed for a period of 10 mins at a steady potential (0.65 V vs Ag/AgCl). Fig. 4.20 shows the current density-time responses of Ni-Cu-Mo/MWCNTs alloy catalysts for methanol electro-oxidation at different temperatures. The two catalysts present a gradual current decay before a constant current status was obtained which was attributed to the formation of some Ni oxides/hydroxides which were adsorbed as intermediates in MOR [37]. As expected, the MOR current flux density of the alloy catalyst calcinated at high temperature was evidently higher than that performed at lower temperature. At steady-state region, it was observed that the alloy catalyst calcinated at high temperature presented current flux density of  $33.80\text{mA}/\text{cm}^2$  Ni (decreased 15.42% relative initial current flux density) while one at lower temperature exhibited current flux density of about  $11.21\text{mA}/\text{cm}^2$  Ni (45.26%). The alloy catalyst calcinated at lower temperature shows the lowest initial current flux density and limiting current flux density which may be due to the conversion of Ni into nickel oxide/hydroxide which have covered the Cu/Mo atoms surface in the polarization process [59].

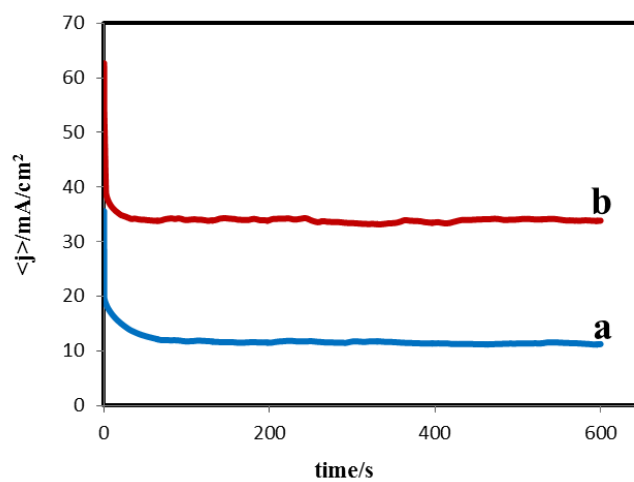


Figure 4.20: Chronoamperometry collected for 10 min at 0.650 V for Ni-Cu-Mo/MWCNTs alloy catalyst at 900°C (a) and 1100°C (b) in 0.5 M  $CH_3OH$  + 0.1 M  $KOH$

## **4.6 Physical Characterization of Ni-Cu-W/MWCNTs**

### **Alloy Catalyst**

The results obtained from various spectroscopic studies as well as electrochemical measurements of Ni-Cu-W/MWCNTs are discussed as follows;

#### **4.6.1 X-Ray Diffraction (XRD) Analysis**

Fig. 4.21 shows the X-ray diffraction (XRD) patterns of the Ni-Cu-W/MWCNTs composite at varying temperatures with broad peaks at  $2\theta = 25.466^\circ$  are associated with the (002) planes of the graphite-like structure of the multi-walled carbon nanotubes. The other three peaks of the Ni-Cu-W/MWCNTs composite corresponds to the planes (111), (200) and (220) at  $2\theta$  values of about  $44.238^\circ$ ,  $51.538^\circ$  and  $75.962^\circ$  respectively which had been well reported in literature [37]. The slight shifts of the diffraction peaks reveal partial Cu and W have entered into the Ni lattice and results to the formation of Ni-Cu-W alloy on the multi-walled carbon nanotubes surface.



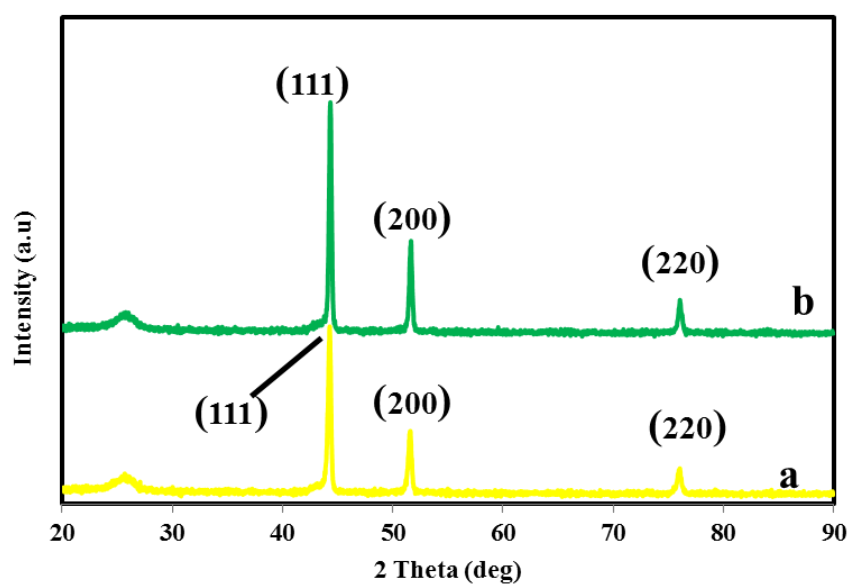


Figure 4.21: X-ray diffraction (XRD) patterns of Ni-Cu-W/MWCNTs alloy catalyst at 900°C (a) and 1100°C (b)

### 4.6.2 FE-SEM Analysis

The FE-SEM micrographs of the highly dispersed Ni-Cu-W/MWCNTs composite and it could be observed that more metal nanoparticles exhibit very well uniform dispersion on the functionalized MWCNTs surface (Fig. 4.22). The images of the synthesized catalysts at higher magnification of  $20\mu m$  scale bar reveal good porous structure which has been found to demonstrate high methanol electro-oxidation activity than the dense ones.

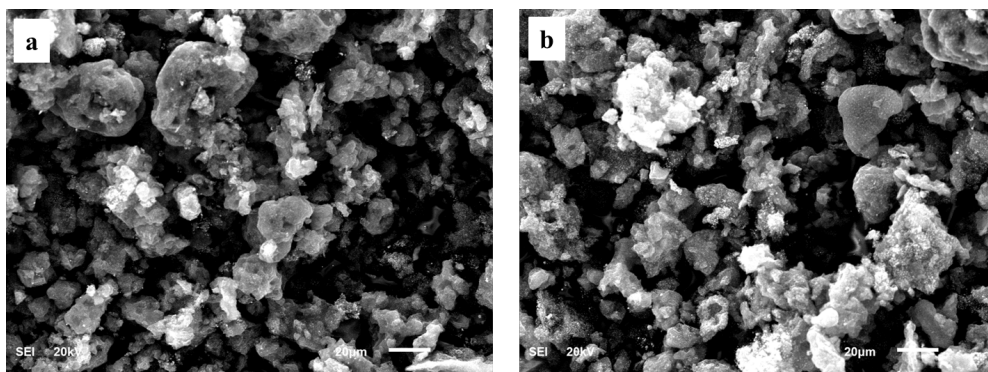


Figure 4.22: SEM micrographs of Ni-Cu-W/MWCNTs alloy catalyst at 900°C (a) and 1100°C (b)

### 4.6.3 Elemental Analysis

**EDX Analysis:** The energy-dispersive X-ray spectroscopy (EDX) analysis (Fig. 4.23) was undertaken to determine the major elements of the synthesized Ni-Cu-W/MWCNTs catalyst. Thus, the EDX spectrum shows peaks of C, Ni, Cu and W which were the synthesized catalyst composition and Table 4.8 and 4.9 shows the percentage composition by weight of the identified elements in the synthesized Ni-Cu-W/MWCNTs composites. Based on the percentage composition given in the tables, the summary of the average value of each element in each catalyst composite is given in Table 4.10.

**Mapping of Ni-Cu-W/MWCNTs alloy catalyst:** The uniform distribution of Ni, Cu and W particles on the MWCNTs support surface was evidenced by elemental mapping using energy-dispersive X-ray spectroscopy attached to FE-SEM JEOL JSM 6610LV machine (Fig. 4.24).

**ICP-MS Analysis:** To further evaluate the Ni, Cu and W chemical component, ICP-MS was used for the estimation of the chemical composition of the MWCNTs supported Ni-Cu-W catalyst. The digestion of the sample was done in aqua regia, filtered and made up to the mark in standard flask with Milli-Pore water as reported in literature [56]. The results of the analysis have shown an agreement between the atomic ratio obtained and that resulted from theoretical calculation for the component elements (i.e Ni, Cu and W) of the alloy catalyst. Thus, the phenomenon further supports the formation of highly dispersed Ni-Cu-W/MWCNTs alloy catalyst.

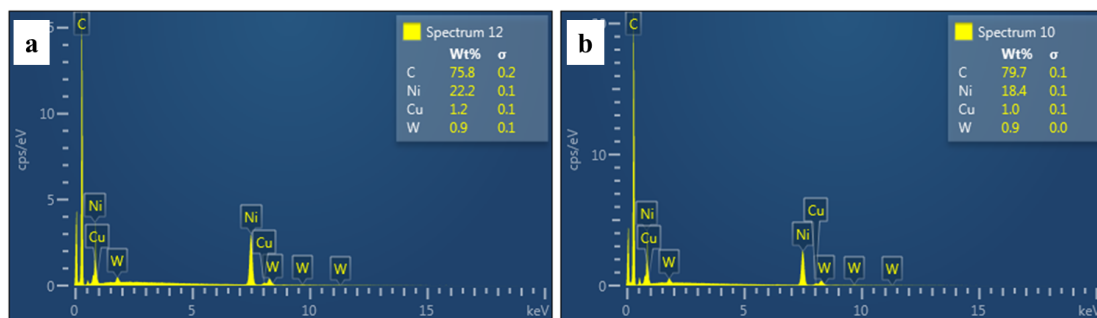


Figure 4.23: EDX Spectrum of Ni-Cu-W/MWCNTs alloy catalyst at 900°C (a) and 1100°C (b)

Table 4.8: EDX Table showing percentage composition of Ni-Cu-W/MWCNTs alloy catalyst at 900°C

Elem	Line Type	App Conc	K Ratio	Wt %	Wt % Sigma	Std Label	Factory Std
C	K Series	73.27	0.73266	75.77	0.15	C Vit	Yes
Ni	K Series	49.57	0.49569	22.16	0.14	Ni	Yes
Cu	K Series	2.47	0.02465	1.16	0.07	Cu	Yes
W	M Series	1.72	0.01724	0.91	0.05	W	Yes
Total				100			

Table 4.9: EDX Table showing percentage composition of Ni-Cu-W/MWCNTs alloy catalyst at 1100°C

Elem	Line Type	App Conc	K Ratio	Wt %	Wt % Sigma	Std Label	Factory Std
C	K Series	86.11	0.86110	79.69	0.13	C Vit	Yes
Ni	K Series	40.95	0.40948	18.44	0.12	Ni	Yes
Cu	K Series	2.0	0.02001	0.95	0.06	Cu	Yes
W	M Series	1.78	0.01783	0.92	0.05	W	Yes
Total				100			

Table 4.10: Summary of the average percent by weight of the elements in each alloy catalyst composite

Catalyst	C	Ni	Cu	W
90%Ni10%CuMWCNTs(900°C)	73.27	49.57	2.47	1.72
90%Ni10%CuMWCNTs(1100°C)	86.11	40.95	2.00	1.78

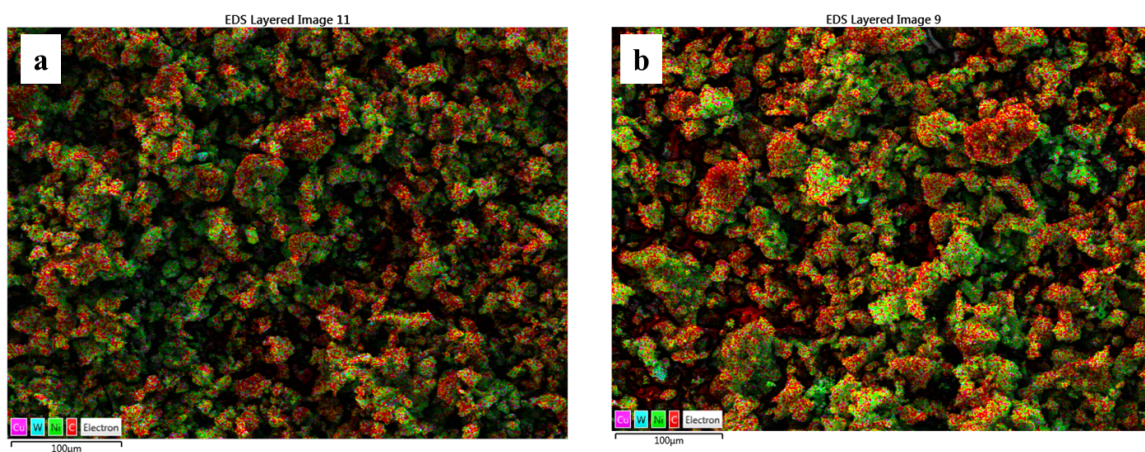


Figure 4.24: Elemental Mapping of Ni-Cu-W/MWCNTs alloy catalyst at 900°C (a) and 1100°C (b)

#### **4.6.4 FE-TEM Analysis**

The synthesized Ni-Cu-W/MWCNTs alloy catalyst composite morphology and particle size distribution on the multi-walled carbon nanotubes support were examined using FE-TEM JEOL JEM-2100F, Japan (Fig. 4.25). The HRTEM micrographs show that the Ni-Cu-W nanoparticles are decorated on the MWCNTs and homogenously dispersed largely in spherical shape. The aggregation of the metal nanoparticles is rarely observed. This is may be due to the specific nucleation sites such as carbonyl, hydroxyl and carboxyl, which aid the metal nanoparticles to be adsorbed at the surface of the MWCNTs through hydrogen bonding [57, 58].



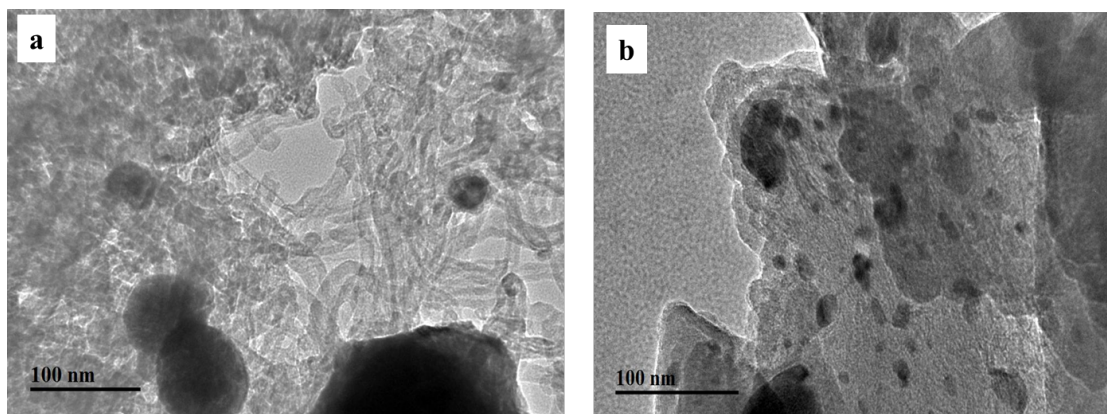


Figure 4.25: HRTEM micrographs of Ni-Cu-W/MWCNTs alloy catalyst at 900°C (a) and 1100°C (b)

## 4.7 Cyclic Voltammogram in $N_2$ saturated solution

Also the same electrochemical measurement was conducted for Ni-Cu-W/MWCNTs alloy catalyst of different temperatures. Fig. 4.26 shows the cyclic voltammetric curves of methanol oxidation (0.5 M) for Ni-Cu-W/MWCNTs electrode formulations of different heat treatments in a -0.2 to 1.0 V potential range (vs Ag/AgCl) at a 20 mV/s scan rate in 0.1 M KOH and Fig. 4.27 shows cyclic voltammograms of Ni-Cu-W/MWCNTs electrode at different temperature in a -0.2 to 1.0 V potential range (Vs Ag/AgCl) at a  $20\text{mV}/s$  scan rate in 0.5 M  $CH_3OH$  + 0.1 M  $KOH$  solution.

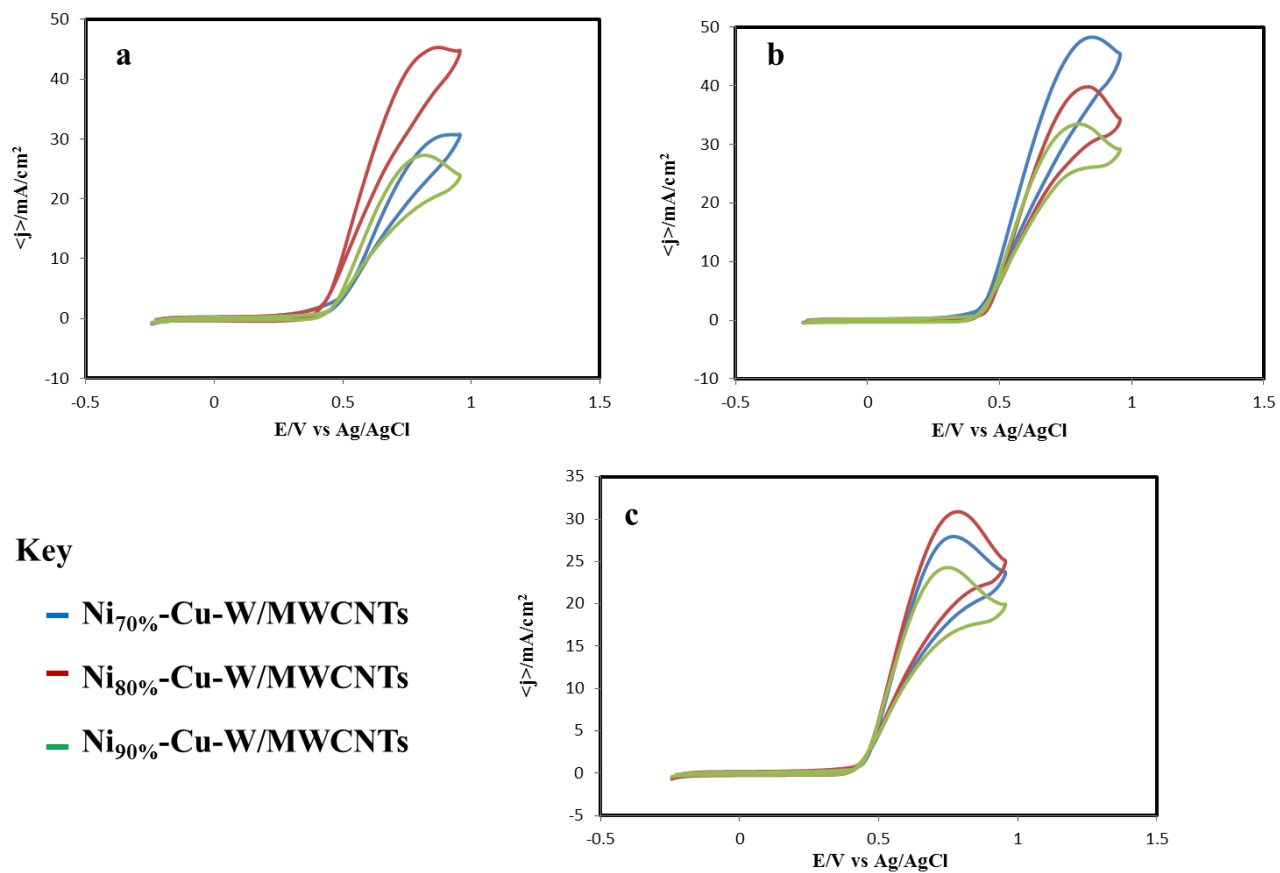


Figure 4.26: Cyclic voltammograms of Ni-Cu-W/MWCNTs electrode formulations at 700 °C (a), 900 °C (b) and 1100 °C (c) in 0.5 M  $CH_3OH$  + 0.1 M  $KOH$  at a scan rate of 20 mV/s

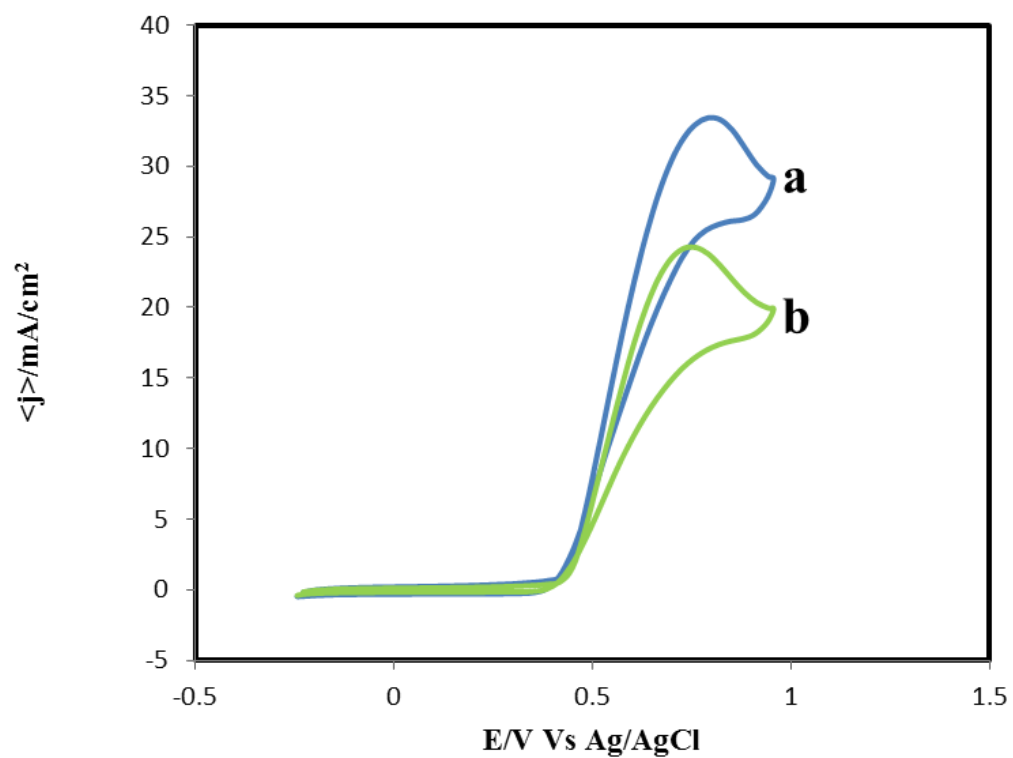


Figure 4.27: Cyclic voltammograms of Ni-Cu-W/MWCNTs electrode at 900 °C (a) and 1100 °C (b) in 0.5 M  $\text{CH}_3\text{OH}$  + 0.1 M  $\text{KOH}$  at a scan rate of  $20\text{mV}/\text{s}$

#### **4.7.1 Effect of Ni-Cu-W/MWCNTs Alloy Catalyst Loading**

The electroactivity of Ni-Cu-W/MWCNTs alloy catalyst in methanol was investigated by conducting cyclic voltammetry in a nitrogen saturated 0.1 M *KOH* solution with catalyst loadings of  $0.2\text{mg}/\text{cm}^2$  and  $0.4\text{mg}/\text{cm}^2$  respectively. The cyclic voltammetric curves obtained are shown in Fig. 4.28. It can be seen that the current flux densities have increased with increasing the catalyst loading and the MOR on-set potentials have no significant change with the catalyst loading at  $900^\circ\text{C}$  and otherwise at  $1100^\circ\text{C}$ . Although, at low catalyst loading the limiting currents were not well-defined but became better as the catalyst loading was increased due to presence of more active sites for methanol oxidation at  $900^\circ\text{C}$ . The high activity obtained during this work especially with Ni-Cu-W/MWCNTs, can be attributed to the addition of synergic metal (W) (co-catalyst) especially at higher catalyst loading

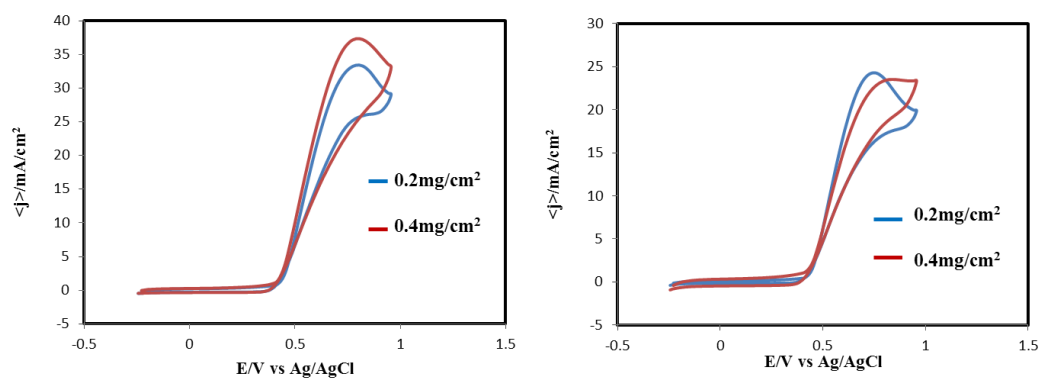


Figure 4.28: Cyclic voltammograms of Ni-Cu-W/MWCNTs catalyst loading at  $900^\circ\text{C}$  (a) and  $1100^\circ\text{C}$  (b) in  $0.5 \text{ M CH}_3\text{OH} + 0.1 \text{ M KOH}$  at a scan rate of  $20 \text{ mV}/\text{s}$

#### **4.7.2 Ni-Cu-W/MWCNTs Alloy Catalyst Durability**

The stability of Ni-Cu-W/MWCNTs alloy catalyst was investigated by potential cycling in 0.1 M *KOH* electrolyte in presence of 0.5 M *CH<sub>3</sub>OH*. The catalyst calcinated at high temperature (1100 °C) has shown remarkable activity in addition good stability after being subjected to prolonged potential cycling between 0.20 and 1.0 V/RHE at a scan rate of 20 mV/s in accordance with the DOE protocol. At a constant current flux density (approximately half-wave potential), it was observed that there is significant drop in the voltage (Fig. 4.29).

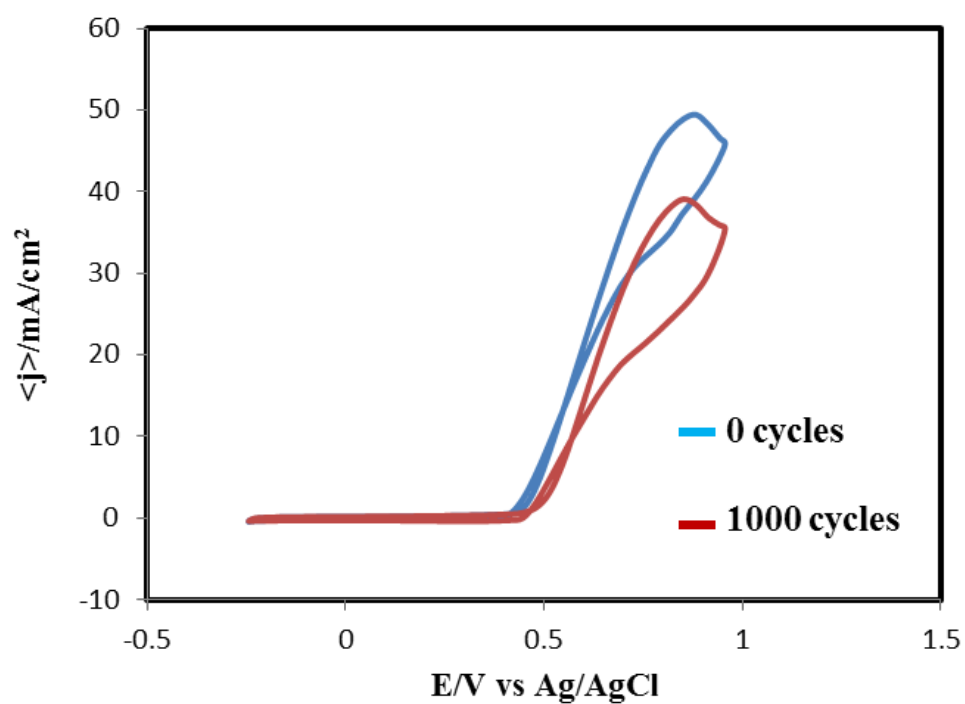


Figure 4.29: Stability Test for Ni-Cu-W/MWCNTs Cyclic Voltammograms in  $N_2$  saturated 0.5 M  $CH_3OH$  + 0.1 M  $KOH$



Chronoamperometry was conducted on the alloy catalyst in order to further evaluate the electrocatalytic activity as well as stability and it was carried out for up to 10 mins at constant potential (0.65 V vs Ag/AgCl). Fig. 4.30 shows the current density-time responses of Ni-Cu-W/MWCNTs alloy catalysts for methanol electro-oxidation at different temperatures. The two catalysts present a gradual current decay before a constant current status was obtained which was attributed to some Ni oxides/hydroxides formation and adsorbed intermediates in MOR [37]. As expected, the MOR current flux density of the alloy catalyst calcinated at high temperature was evidently higher than that of the one at lower temperature. At steady-state region, it was observed that the alloy catalyst calcinated at high temperature presented current flux density of  $26.70\text{mA}/\text{cm}^2$  Ni (decreased 22.54% relative initial current flux density) after 10 min while one at lower temperature exhibited current flux density of about  $9.77\text{mA}/\text{cm}^2$  Ni (43.33%). The alloy catalyst calcinated at lower temperature shows the lowest initial current flux density and limiting current flux density which may be due to the conversion of Ni into nickel oxide/hydroxide which have covered the Cu/W atoms surface in the polarization process [59].

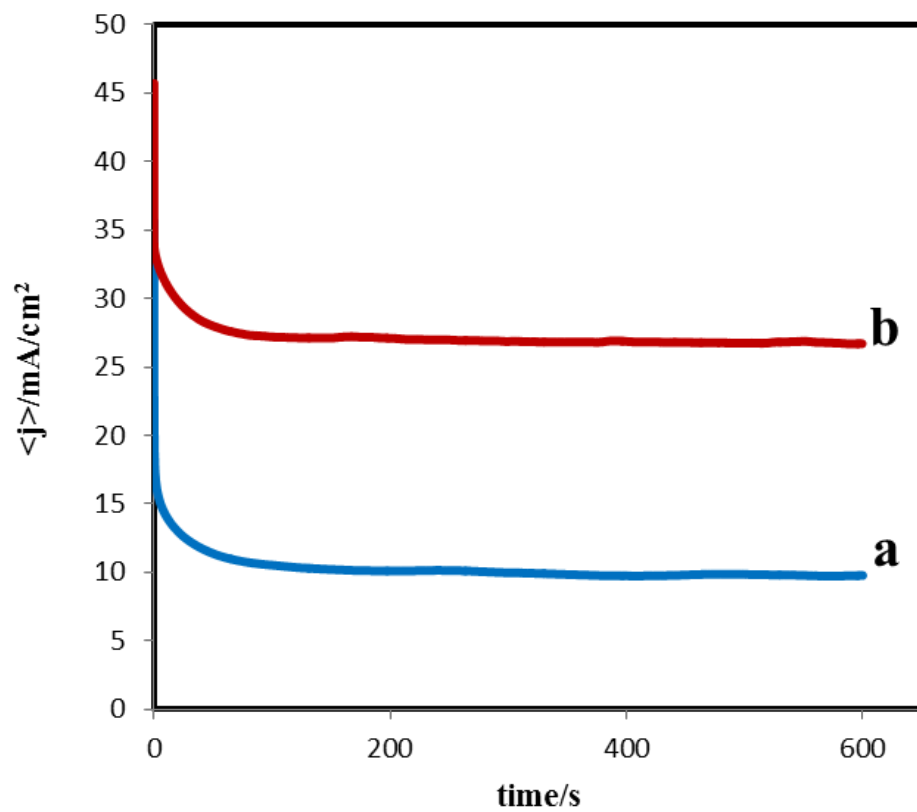


Figure 4.30: Chronoamperometry collected for 10 min at 0.650 V for Ni-Cu-W/MWCNTs alloy catalyst at 900°C (a) and 1100°C (b) in 0.5 M  $CH_3OH$  + 0.1 M  $KOH$

## CHAPTER 5

# CONCLUSION AND RECOMMENDATIONS

In this work, several catalysts for the oxidation of methanol were synthesized, characterized and their activity tested. The following are the scientific contributions:

1. A novel MWCNTs supported Ni-Cu and Ni-Cu-X ( $X = \text{Mo/W}$ ) were first synthesized for MOR by sequential wet impregnation method combined with a freezing drying procedure.
2. The binary Ni-Cu/MWCNTs alloy catalysts showed moderate electro-catalytic activity and stability towards methanol oxidation.
3. The ternary Ni-Cu-X/MWCNTs ( $X=\text{Mo/W}$ ) alloy catalysts showed superior electro-catalytic activity and stability towards methanol oxidation.
4. The Ni-Cu/MWCNTs and Ni-Cu-X ( $X=\text{Mo/W}$ ) alloy catalysts demonstrated a Pt-like behavior in the alkaline medium.

5. The variations of the heat treatment temperatures of the synthesized catalysts in order to obtain an optimum performing catalysts.

Therefore, it can be concluded that the objectives outlined for this work have been successfully achieved. As summarized above, present study was focused on the selection of proper carbon supports as well as the synthesis method for the production of non-precious metals electrocatalysts used in the fuel cells technologies. Though, this work has covered many of the most essential properties of the electrocatalysts, however much still needed to be done to cover areas which have not been covered in this work. Thus, the following recommendations are made for future work:

1. The use of carbon nanotubes extensively as an active surface support for Pt-free anode catalysts.
2. The use of the novel method of synthesis used in this work because it greatly prevents particles agglomeration.
3. The incorporation of co-catalysts (such as Mn, Co) into the binary alloy catalyst so as to further enhance their catalytic performance.
4. The reduction in the metals loading on the carbon support.
5. Extensive study on possible commercialization of the synthesized electrocatalysts.

# REFERENCES

- [1] Fuel Cell Today, the leading authority on fuel cells. <http://www.fuelcelltoday.com/>
- [2] <http://www.fuelcellenergy.com/why-fuelcell-energy/benefits/>
- [3] <http://www.heliocentris.com/en/academia-offering/information/technology-guide/fuel-cell.html>.
- [4] Slade R, Varcoe J (2005) Investigations of conductivity in FEP-based radiation-grafted alkaline anion-exchange membranes. *Solid State Ionics* 176:585-597.
- [5] Yu EH, Scott K (2004) Direct methanol alkaline fuel cell with catalysed metal mesh anodes. *Electrochem commun* 6:361-365.
- [6] Wasmus S, Ku A (1999) Methanol oxidation and direct methanol fuel cells: a selective review 1. 461:1431.
- [7] Zhao Y, Fan L, Ren J, Hong B (2014) Electrodeposition of PtRu and PtRuNi nanoclusters on multi-walled carbon nanotubes for direct methanol fuel cell. *Int J Hydrogen Energy* 39:4544-4557.

- [8] Gasteiger HA, Markovi N, Ross PN, Cairns EJ (1993) Methanol electrooxidation on well-characterized Pt-Ru alloys. *J Phys Chem* 97:12020-12029.
- [9] Frelink T, Visscher W, van Veen J a. R (1995) Particle size effect of carbon-supported platinum catalysts for the electrooxidation of methanol. *J Electroanal Chem* 382:65-72.
- [10] Zhao Q, Gan Z, Zhuang Q (2002) Electrochemical Sensors Based on Carbon Nanotubes. *Electroanalysis* 14:1609-1613.
- [11] Finnerty CM, Coe NJ, Cunningham RH, Ormerod RM (1998) Carbon formation on and deactivation of nickel-based/zirconia anodes in solid oxide fuel cells running on methane. *Catal Today* 46:137-145.
- [12] Scott K, Yu E (2009) Electrocatalysis in the Direct Methanol Alkaline Fuel Cell. 487-525.
- [13] Finnerty CM, Coe NJ, Cunningham RH, Ormerod RM (1998) Carbon formation on and deactivation of nickel-based/zirconia anodes in solid oxide fuel cells running on methane. *Catal Today* 46:137-145.
- [14] Ishihara T, Yan J, Shinagawa M, Matsumoto H (2006) NiFe bimetallic anode as an active anode for intermediate temperature SOFC using *LaGaO<sub>3</sub>* based electrolyte film. *Electrochim Acta* 52:1645-1650.
- [15] Gorte RJ, Park S, Vohs JM, Wang C (2000) Anodes for direct oxidation of dry hydrocarbons in a solid-oxide fuel cell. *Adv Mater* 12:1465–1469.

- [16] Kim H, Lu C, Worrell WL, et al. (2002) Cu-Ni Cermet Anodes for Direct Oxidation of Methane in Solid-Oxide Fuel Cells. *J Electrochem Soc* 149:A247.
- [17] Kan H, Hyun SH, Shul Y-G, Lee H (2009) Improved solid oxide fuel cell anodes for the direct utilization of methane using Sn-doped Ni/YSZ catalysts. *Catal Commun* 11:180-183.
- [18] Nabae Y, Yamanaka I, Hatano M, Otsuka K (2008) Mechanism of Suppression of Carbon Deposition on the *PdNi/Ce(Sm)O<sub>2</sub> La(Sr)CrO<sub>3</sub>* Anode in Dry CH<sub>4</sub> Fuel. *J Phys Chem C* 112:10308-10315.
- [19] Van Effen RM, Evans DH, A WUS (1979) *J. Electroanal, Chem.*, 103:383–397
- [20] Costamagna P, Srinivasan S (2001) Quantum jumps in the PEMFC science and technology from the 1960s to the year 2000 Part I . Fundamental scientific aspects 102:242-252.
- [21] Wee J-H, Lee K-Y, Kim SH (2007) Fabrication methods for low-Pt-loading electrocatalysts in proton exchange membrane fuel cell systems. *J Power Sources* 165:667-677.
- [22] Aric AS, Baglio V, Antonucci V (2009) Direct Methanol Fuel Cells: History, Status and Perspectives.
- [23] Cathro KJ (1969) The Oxidation of Water-Soluble Organic Fuels Using Platinum-Tin Catalysts. *J Electrochem Soc* 116:1608.

- [24] Watanabe M, Motoo S (1975) *Electroanalytical Chemistry and Interfacial Electrochemistry*, 60:275-283.
- [25] Bagotzky VS, Vassilyev YB (1967) MECHANISM OF ELECTRO-OXIDATION OF METHANOL ON THE PLATINUM ELECTRODE 12:1323-1343.
- [26] Parsons R, Vandernoot T (1988) The oxidation of small organic molecules A survey of recent fuel cell related research. 257:9-45.
- [27] Aramata A, Kodera T, Masuda M (1988) Electrooxidation of methanol on platinum bonded to the solid polymer electrolyte, Nafion. *J Appl Electrochem* 18:577-582.
- [28] Fleischmann M, Korinek K, Pletcher D (1971) The formation of adsorbed hydrogen radicals. 31:39-49.
- [29] McNicol B., Rand DA., Williams K. (1999) Direct methanol-air fuel cells for road transportation. *J Power Sources* 83:15-31.
- [30] Poirier JA (1994) Microstructural Effects on Electrocatalytic Oxygen Reduction Activity of Nano-Grained Thin-film Platinum in Acid Media. *J Electrochem Soc* 141:425.
- [31] Watanabe M, Saegusa S, Stonehart P (1989) High platinum electrocatalyst utilizations for direct methanol oxidation. *J Electroanal Chem Interfacial Electrochem* 271:213-220.



- [32] Taraszewska J, Rosonek G (1994) Electrocatalytic oxidation of methanol on a glassy carbon electrode modified by nickel hydroxide formed by ex situ chemical precipitation. *J Electroanal Chem* 364:209-213.
- [33] Abdel Rahim MA, Abdel Hameed RM, Khalil MW (2004) Nickel as a catalyst for the electro-oxidation of methanol in alkaline medium. *J Power Sources* 134:160-169.
- [34] Sanches LS, Domingues SH, Marino CEB, Mascaro LH (2004) Characterisation of electrochemically deposited NiMo alloy coatings. *Electrochem commun* 6:543-548.
- [35] Zhao Y, E Y, Fan L, et al. (2007) A new route for the electrodeposition of platinumnickel alloy nanoparticles on multi-walled carbon nanotubes. *Electrochim Acta* 52:5873-5878.
- [36] Hameed RMA, El-Khatib KM (2010) NiP and NiCuP modified carbon catalysts for methanol electro-oxidation in KOH solution. *Int J Hydrogen Energy* 35:2517-2529.
- [37] Zhao Y, Yang X, Tian J, et al. (2010) Methanol electro-oxidation on Ni@Pd core-shell nanoparticles supported on multi-walled carbon nanotubes in alkaline media. *Int J Hydrogen Energy* 35:3249-3257.
- [38] Awasthi R, Singh RN (2010) Synthesis and Characterization of Nano Structured Pd-Ni and Pd-Ni-C Composites Towards Electrooxidation of Alcohols. 70-78.

- [39] Antolini E, Gonzalez ER (2010) Tungsten-based materials for fuel cell applications. *Appl Catal B Environ* 96:245-266.
- [40] Tong X, Qin Y, Guo X, et al. (2012) Enhanced Catalytic Activity for Methanol Electro-oxidation of Uniformly Dispersed Nickel Oxide Nanoparticles-Carbon Nanotube Hybrid Materials. *Small* 3390-3395.
- [41] Altunba ahin E, Karda G (2013) Cobalt-modified nickelzinc catalyst for electrooxidation of methanol in alkaline medium. *J Solid State Electrochem* 17:2871-2877.
- [42] Amin RS, Abdel Hameed RM, El-Khatib KM, Elsayed Youssef M (2014) Electrocatalytic activity of nanostructured Ni and PdNi on Vulcan XC-72R carbon black for methanol oxidation in alkaline medium. *Int J Hydrogen Energy* 39:2026-2041.
- [43] Amin RS, Hameed RMA, ElKhatib KM (2014) Microwave heated synthesis of carbon supported Pd, Ni and PdNi nanoparticles for methanol oxidation in KOH solution. *Appl Catal B Environ* 148-149:557-567.
- [44] Ravikumar MK (1996) Effect of Methanol Crossover in a Liquid-Feed Polymer-Electrolyte Direct Methanol Fuel Cell. *J Electrochem Soc* 143:2601.
- [45] Merzougui B, Hachimi A, Akinpelu A, et al. (2013) A Pt-free catalyst for oxygen reduction reaction based on FeN multiwalled carbon nanotube composites. *Electrochim Acta* 107:126–132.
- [46] Dresselhaus MS, Dresselhaus G, Avouris P (2001) Carbon Nanotubes.

- [47] Thostenson ET, Ren Z, Chou T-W (2001) Advances in the science and technology of carbon nanotubes and their composites: a review. *Compos Sci Technol* 61:1899-1912.
- [48] Amelinckx S, Lucas A, Lambin P (1999) Electron diffraction and microscopy of nanotubes. *Reports Prog Phys* 62:1471-1524.
- [49] Shao Y, Yin G, Zhang J, Gao Y (2006) Comparative investigation of the resistance to electrochemical oxidation of carbon black and carbon nanotubes in aqueous sulfuric acid solution. *Electrochim Acta* 51:5853-5857.
- [50] Wang X, Li W, Chen Z, et al. (2006) Durability investigation of carbon nanotube as catalyst support for proton exchange membrane fuel cell. *J Power Sources* 158:154-159.
- [51] Yu R, Chen L, Liu Q, et al. (1998) Platinum Deposition on Carbon Nanotubes via Chemical Modification. *Chem Mater* 10:718-722.
- [52] Hou Y, Gao S (2003) Monodisperse nickel nanoparticles prepared from a monosurfactant system and their magnetic properties Electronic supplementary information (ESI) available: XPS of Ni nanoparticles; plot of magnetization vs. applied field. <http://www.rsc.org/suppdata/jm>. *J Mater Chem* 13:1510.
- [53] Prabhuram J, Zhao TS, Tang ZK, et al. (2006) Multiwalled carbon nanotube supported PtRu for the anode of direct methanol fuel cells. *J Phys Chem B* 110:5245-52.

- [54] Guo G, Qin F, Yang D, et al. (2008) Synthesis of Platinum Nanoparticles Supported on Poly(acrylic acid) Grafted MWNTs and Their Hydrogenation of Citral. *Chem Mater* 20:2291-2297.
- [55] Casella IG, Guascito MR, Sannazzaro MG (1999) Voltammetric and XPS investigations of nickel hydroxide electrochemically dispersed on gold surface electrodes. *J Electroanal Chem* 462:202-210.
- [56] Lee S, Kim HJ, Choi SM, et al. (2012) The promotional effect of Ni on bimetallic PtNi/C catalysts for glycerol electrooxidation. *Appl Catal A Gen* 429-430:39-47.
- [57] Yang D-Q, Sun S, Dodelet J-P, Sacher E (2008) A Facile Route for the Self-Organized High-Density Decoration of Pt Nanoparticles on Carbon Nanotubes. *J Phys Chem C* 112:11717-11721.
- [58] Chen J, Wang M, Liu B, et al. (2006) Platinum catalysts prepared with functional carbon nanotube defects and its improved catalytic performance for methanol oxidation. *J Phys Chem B* 110:11775-9.
- [59] Domnguez-Crespo M, Ramrez-Meneses E, Montiel-Palma V, et al. (2009) Synthesis and electrochemical characterization of stabilized nickel nanoparticles. *Int J Hydrogen Energy* 34:1664-1676.

## Vitae

**Name** : Olanrewaju Suleiman Olakunle

**Nationality** : Nigerian

**E-mail address** : lakunlepolymer@yahoo.com

**Present Address** : Department of Chemistry, King Fahd University of Petroleum & Minerals, Dhahran, 31261, Saudi Arabia.

**Permanent Address** : 1A Social Science Road Unilag Estate Magodo GRA Lagos State, Nigeria.

**Tel. Number** : +966531529012/+2348032182510

### Academic Background

**M.Sc.**, Chemistry,

King Fahd University of Petroleum and Minerals, Dhahran, Saudi Arabia.

**B.Sc.**, Chemistry (with Polymer Science),

Federal University of Technology, Minna, Nigeria.

### Academic Publications

**O.S Olakunle**, A. Al-Ahmed, B. Merzougui, A. Abulkibash, A. S. Sultan, J. Zaidi;

“Highly Dispersed Ni-Cu Anode Catalyst for Alkaline DMFC”, *Electrochim Acta* (submitted) 2015.

J.O Tijani, M.M Ndamitso, I.B Aliyu, **O.S Olakunle**; “Equilibrium and Isotherm Studies of Biosorption of Potentially Toxic Elements from Aqueous Solution By *Blighia sapida* (Akee apple) Seeds”, *Int. Journal of Advancements Research and Tech. (IJOART)* **2013**, 2(3), 1-12.